Lattice QCD: a critical status report

Karl Jansen[*]

DESY,
Platanenallee 6, 15738 Zeuthen, Germany
E-mail: `Karl.Jansen@desy.de`

The substantial progress that has been achieved in lattice QCD in the last years is pointed out. I compare the simulation cost and systematic effects of several lattice QCD formulations and discuss a number of topics such as lattice spacing scaling, applications of chiral perturbation theory, non-perturbative renormalization and finite volume effects. Additionally, the importance of demonstrating universality is emphasized.

---

[*]Speaker.

1. Introduction

At the Capri lattice symposium in 1989, it was stated that in lattice field theory it would have been necessary *"both a 10^8 increase in computing power AND spectacular algorithmic advances before a useful interaction with experiments starts taking place."* [1]. At the time of this statement, in 1989, the available computing power was around $10 - 100$Gigaflops [2]. As a consequence, lattice field theory would have needed at least Exaflops computers in order to perform realistic simulations and to produce any experimentally interesting output.

In addition, at the lattice conference in Berlin in 2001 a serious attempt to determine the scaling behaviour of the algorithms to simulate lattice QCD as a function of the quark mass, the lattice spacing and the volume was made. It was found [3, 4] that the expense of lattice QCD simulations increases with a large inverse power of the quark mass leading to exorbitant costs at the physical value of the pseudo scalar mass, which we will denote as the physical point further on. In fact, the simulations costs turned out to be already very large much before being able to reach the physical point such that simulations with pseudo scalar masses below, say, 300MeV seemed to be completely out of reach.

However, in stark contrast to the above rather pessimistic scenario, it could be witnessed at Lattice 2008 in Williamsburg that a number of lattice QCD simulations with pseudo scalar masses well below 300MeV, values of the lattice spacings down to $a \approx 0.05$fm and box sizes with linear extent $\gtrsim 2.5$fm are currently being performed by various international collaborations. Such simulations allow then for an extrapolation of the results to the physical point and to the continuum limit while keeping also the finite volume effects under control. And, there are even more ambitious simulations starting presently which are performed at or very close to the physical point [5].

Thus, the prognosis which emerged in 1989 has *not* been fulfilled: already nowadays completely realistic simulations of lattice QCD are possible on available machines delivering a few 100 Teraflops. The values of the lattice spacings and pseudo scalar masses which are employed in todays simulations are compiled in fig. 1. In the figure, the blue dot indicates the physical point. The black cross represents a state of the art simulation in the year 2001. As can be seen in the graph, most of the simulations now go well beyond what could be reached in 2001 demonstrating clearly the progress in performing realistic simulations.

This phase transition-like change in the situation is due to three main developments: *i*) algorithmic breakthroughs that either shifted the wall of the algorithm scaling in the quark mass or even changed this scaling behaviour itself drastically, *ii*) machine development; the computing power of the present BG/P systems is even outperforming Moore's law, *iii*) conceptual developments, such as the use of improved actions which reduce lattice artefacts and the development of non-perturbative renormalization.

To illustrate the status of present lattice QCD simulations let me give just two examples for the results obtained at the moment.

1.1 Baryon spectrum

When simulations of lattice QCD were started, the computation of the baryon spectrum was one of the main goals. Although such a computation can only be considered as a post diction since
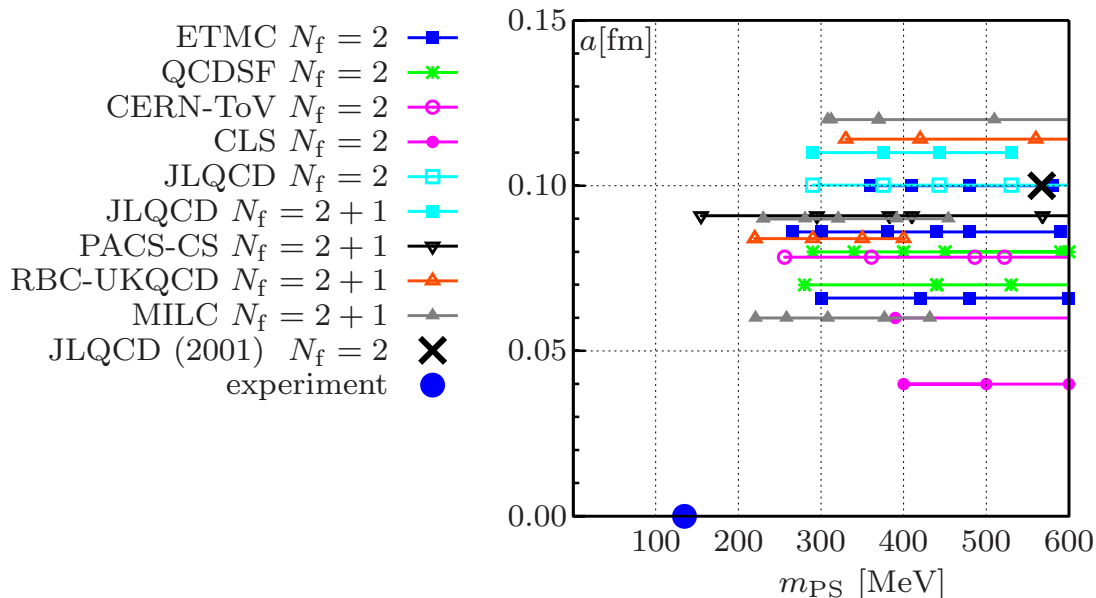
Figure 1: The values of the lattice spacing *a* and pseudo scalar masses m_{PS} as employed presently in typical QCD simulations by various collaborations as (incompletely) listed in the legend. The blue dot indicates the physical point where in the continuum the pseudo scalar assume assumes its experimentally measured value. The black cross represents a state of the art simulation by the JLQCD collaboration in 2001.

the masses are measured precisely in experiment, their determination on the lattice has always been considered as an important benchmark calculation.

　　It is very reassuring that many international collaborations working with lattice field theoretical methods are either very close to finish the computation of the baryon spectrum [6, 7, 8, 9, 10, 11, 12] or, as in the case of the Budapest-Marseille-Wuppertal collaboration have already accomplished the goal [13]. In fig. 2 the recent results from the BMW-collaboration presented at this conference is shown.

　　In order to obtain the baryon spectrum shown in the graph, simulations at three different values of the lattice spacing 0.065fm $\lesssim a \lesssim$ 0.125fm have been performed. The values of the pseudo scalar masses are bracket by 200MeV $\lesssim m_{PS} \lesssim$ 500MeV. Finally, the box size has been chosen such that $m_{PS}L \gtrsim 4$. This setup allows for extrapolations to the physical point. It also allows for a continuum limit extrapolation and suppresses finite volume effects for many quantities. Thus, the spectrum calculation shown in fig. 2 can be considered as a first lattice benchmark calculation with, however, the caveat of the need for an eventual cross-check. Nevertheless, the agreement of the lattice results with the experimentally measured Baryon spectrum is highly non-trivial.

　　The work of ref. [13] is a lattice computation from only one group and from only one lattice discretization. In order to say with confidence that this is a direct non-perturbative *QCD* result, it is mandatory, in my opinion, that the computation is repeated by at least one different collaboration with most preferably a different lattice action. Only then we will have demonstrated that lattice methods provide a reliable tool to obtain physical results from first principles and in a non-perturbative fashion.

　　The reason for additional calculations of physical quantities is that different lattice formula-
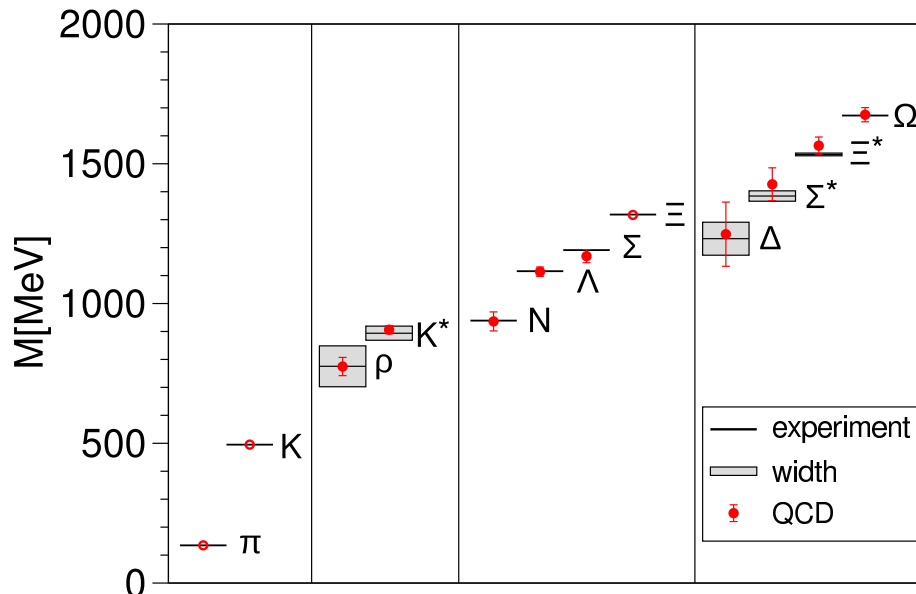
Figure 2: The Baryon spectrum as obtained by the Budapest-Marseille-Wuppertal collaboration [13].

tions of QCD will show different systematic errors and only the continuum limit will reveal whether consistent results are obtained, thus demonstrating non-perturbatively that universality is realized. This point is further discussed below. There it will be demonstrated that for the baryon masses different discretizations indeed seem to give the same continuum limit values. However, for other quantities the situation is much less clear which presumably just means that we need to understand better the inherent systematic effects in our lattice simulations.

1.2 Low energy constants

Another field where a substantial progress could be achieved is the determination of low energy constants of chiral perturbation theory. In the past such determinations were blocked by the expense of performing dynamical fermion simulations with pseudo scalar masses of 300MeV or lower.

With the advances in lattice field theory in recent years, pseudo scalar mass values of $m_{\rm PS} \approx$ 300MeV are simulated today by a number of collaborations as shown in fig. 1. In particular, many collaborations now have very precise results for the pseudo scalar masses and decay constants for $250{\rm MeV} \lesssim m_{\rm PS} \lesssim 450{\rm MeV}$. The existing data show strong indications, at least for the case of $N_f = 2$ flavours of quarks, that chiral perturbation theory is applicable in this regime of corresponding quark masses.

Thus, fits to formulae from chiral perturbation to the very accurate numerical data allow for the determination of the low energy constants of chiral perturbation theory with a high precision. In fig. 3 two examples for fits to formulae from chiral perturbation theory are given. The first example is from the European Twisted Mass collaboration (ETMC) [14, 15, 16]. It shows the pseudo scalar decay constant as a function of the renormalized quark mass, both in units of r_0. In the range of the fit, indicated by the two vertical dotted lines, both, the next to leading order (NLO) and the next to next leading order (NNLO) curves are shown. There is no sensitivity to the NNLO corrections and the NLO formula describes the data very well.
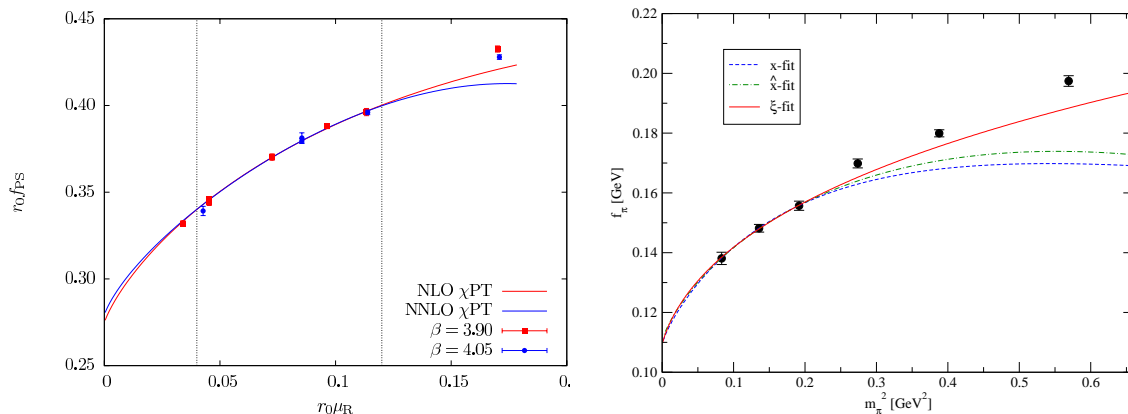
(a) Results from the European twisted mass collaboration (ETMC) comparing NLO and NNLO chiral perturbation theory fits to their numerical data at two values of the lattice spacing, $a \approx 0.085$ fm ($\beta = 3.9$) and $a \approx 0.075$ fm ($\beta = 4.05$). In the fit region, covering pseudo scalar masses between 250MeV and 450MeV no sensitivity to the NNLO correction can be detected.

(b) Results from the Japanese lattice QCD (JLQCD) collaboration. The different expansion parameters are: $x = \frac{2B_0 m_q}{(4\pi f)^2}$, $\hat{x} = (\frac{m_\pi}{4\pi f})^2$ and $\xi = (\frac{m_\pi}{4\pi f_\pi})^2$.

Figure 3: Confronting lattice QCD results for the pseudo scalar decay constant with chiral perturbation theory.

In fig. 3(b) another example, taken from the Japanese lattice QCD (JLQCD) collaboration [17], is given again for the case of the pseudo scalar decay constant. A comparison is made using different expansion parameters for the chiral fit formula. For pseudo scalar masses of $m_{\mathrm{PS}} \lesssim 500$MeV all fits agree indicating again that for such a range of pseudo scalar masses chiral perturbation theory is applicable. We will discuss chiral perturbation theory fits and possible problems below again.

2. Cost of simulation

For sure, conceptual developments – such as O(a)-improvement or non-perturbative renormalization – and new supercomputer architectures are playing an important role for the breakthrough advances in lattice QCD described above. However, the major factor in this development is due to substantial advances in the algorithms that are used to perform our lattice QCD simulations. In fig. 4(a) we show the cost to produce 1000 independent configurations on a lattice of linear size of $L = 2.1$fm with a value of the lattice spacing of $a = 0.08$fm. Although the physical size of the considered box is, by today's standards, not very ambitious, it is chosen in order to compare with the situation at the Lattice symposium 2003 in Tsukuba [4]. There, it was shown that a Wilson fermion simulation at a renormalized quark mass of about 20MeV (in the $\overline{\mathrm{MS}}$-scheme at scale 2GeV) would have needed an unrealistic amount of computer resources. The progress that took place in the last years is illustrated in fig. 4(a). Note that all the cost data were scaled to match a lattice time extend of $T/a = 40$. In fig. 4(a) it is also shown that simulations with staggered fermions were much faster in 2003 than corresponding Wilson fermion simulations.

The situation as of today is summarized in fig. 4(b). The red squares in the graph of fig. 4(a) correspond to measured performance costs from maximally twisted mass fermions (TM) using the
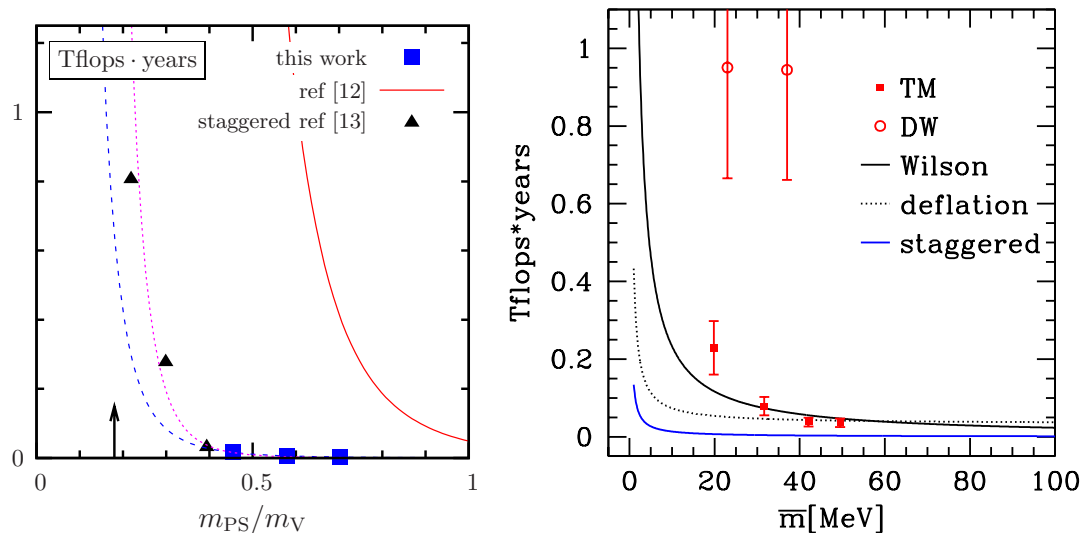
(a) A comparison of the cost estimate taken from ref. [18]. The solid line [23] (indicated as ref. 12 in the plot) indicates the cost of simulations around the time of the Berlin lattice symposium in 2001. The data represented by the filled squares are extrapolated with $(m_{PS}/m_V)^{-4}$ (dashed) and with $(m_{PS}/m_V)^{-6}$ (dotted), respectively. The arrow indicates the physical pion to rho meson mass ratio. Additionally, points from staggered simulations were used for the corresponding plot taken from ref. [4].

(b) The cost of dynamical fermion simulations using different kind of algorithms and lattice fermions. TM stands for twisted mass and data are taken from [18]. DW are domain wall fermions and the performance figures are from [24]. The Wilson performance line is taken from ref. [20], the Wilson performance line using also the deflation technique of ref. [25] is shown as the dotted line. Finally, the staggered performance cost [21] using the algorithm of ref. [22] is represented by the lowest lying (blue) line.

Figure 4: The Berlin wall plots.

algorithm described in [18]. These costs compare nicely with the performance figure for Wilson fermions using the DD-HMC algorithm [19] shown as the solid black line which uses the cost formula,

$$C_{\text{op}} = k \left(\frac{20 \text{ MeV}}{\bar{m}} \right)^{c_m} \left(\frac{L}{3 \text{ fm}} \right)^{c_L} \left(\frac{0.1 \text{ fm}}{a} \right)^{c_a} \text{Teraflops} \times \text{years} \qquad (2.1)$$

with parameters as given in ref. [20]. In eq. (2.1), $\bar{m}$ is the renormalized quark mass at a scale of 2GeV in the $\overline{\text{MS}}$-scheme. Typical values for the exponents in this formula are $c_m = 1-2$, $c_L = 4-5$ and $c_a = 4-6$. Note that these values have a large uncertainty and should here only be taken as a guideline. The prefactor k is typically $O(1)$ for Wilson fermions using the algorithms described in [19, 18] and $O(0.01)$ for staggered fermions [21] when the algorithm of ref. [22] is employed. The performance results for Wilson fermions using the above mentioned algorithms show a tremendous gain when compared to the situation in 2003 [4], see fig. 4(a).

However, this is not even the end of the story. The dotted black line in fig. 4(b) shows the effect of using in-exact eigenvalue deflation of the lattice Dirac operator as described in ref. [25]. As can be observed, the cost is almost flat as a function of the quark mass and the wall-like behaviour sets in only at values of the quark mass below 5MeV. This striking result is even beaten by simulation costs of staggered fermions [21] which are again a noticeable factor below the cost of the best Wilson

fermion simulation. It should be stressed that the lines representing deflated Wilson and staggered fermions are fitting curves that are based on measured performance costs for values of $\bar{m} \gtrsim 20\text{MeV}$ only. For completeness, in the graph the simulation costs [26, 9] of domain wall fermions are also plotted [24]. As can be seen, this formulation of lattice fermions, although requiring an extra dimension, is only moderately more expensive than the one for Wilson formulations. Note that in principle deflation techniques can also be applied to twisted mass, domain wall and staggered fermions, leading possibly to similarly large gains as for Wilson fermions.

In conclusion, the Berlin Wall that was frightening the lattice community in 2001/2003 has been shifted to such small values of the quark mass that for all practical simulations a realistic amount of computer time is needed which matches the capacity of modern supercomputers such as BG/P. (See [27] for an overview of present supercomputer architectures.) Typical physical situations of today are boxes with $L = 3\text{fm}$ and pseudo scalar masses of 200MeV or even 140MeV. Living in a time where a number of machines are available that reach several hundreds of Teraflops or even Petaflops, we will see therefore in the near future many precise and phenomenologically relevant results from the lattice. Of course, if physical problems are to be addressed that need large boxes with $L > 4\text{fm}$ or small values of the lattice spacing with $a < 0.05\text{fm}$, the computing expense will again be beyond present capabilities. Therefore, there is still the need for further developing algorithms and machines for lattice QCD.

Whether simulations are performed directly at the physical point or whether chiral perturbation theory will be used to extrapolate to the physical point is a decision left to the particular collaboration performing such simulations. It is my belief, however, that we need both approaches and that we should understand the mass dependence of physical observables. There is a number of examples, e.g., moments of parton distribution functions, where the present results at about $m_{\text{PS}} = 300\text{MeV}$ are still pretty far away from the experimental value and it will be very interesting to see how the approach to the physical point is realized, as this can provide a valuable insight into the physics of the considered problem. In addition, precise determinations of the low energy constants of chiral perturbation theory from the mass dependence of physical observables will be one of the main accomplishments of lattice QCD.

3. Universality

A demonstration of universality of lattice QCD, i.e. showing that different lattice fermion formulations give consistent continuum limit values for physical observables, is, in my opinion, a crucial goal. Basically all present formulations of lattice QCD have some kinds of conceptual weaknesses (or are too expensive to simulate) leading to different kind of systematic effects which will (hopefully) disappear in the continuum limit. Checking that alternative lattice fermion formulations give consistent results in the continuum limit –and thus demonstrating universality– is hence of utmost importance.

Let me illustrate this point with the example of the Schwinger model taken from ref. [28]. In fig. 5 the continuum limit extrapolation of the mass of the lightest pseudo scalar particle, denoted here as M_π, in the Schwinger model is shown. In this super-renormalizable model the coupling $\beta \propto 1/a^2$ can be used as scaling variable and $M_\pi \sqrt{\beta}$ has a well defined continuum limit for a fixed physical quark mass, i.e. $m_{\text{quark}} \sqrt{\beta}$ fixed. The graph in fig. 5 shows an example of the continuum
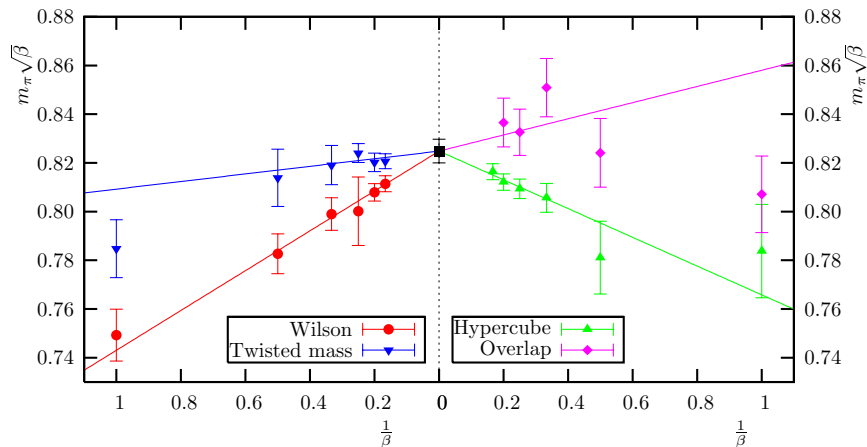
Figure 5: Schwinger model results for the lightest pseudo scalar particle mass $\sqrt{\beta}M_\pi$ as a function of $a^2 = 1/\beta$. The continuum limit scaling is shown for Wilson, maximally twisted mass, hypercube and overlap fermions for a fixed value of the quark mass. The common continuum limit value for all these kind of lattice fermions demonstrates universality for this model.

limit for one choice of a fixed quark mass using Wilson [29], maximally twisted mass [30], hypercube [31] and overlap fermions [32]. Taken aside the overlap fermion simulations which have too large errors to be really conclusive, all formulations show the expected a^2 scaling behaviour and converge to the same continuum limit value thus demonstrating nicely universality.

In my opinion, it would be most important to have analogous graphs for various quantities in case of lattice QCD demonstrating convincingly that we can obtain consistent results in the continuum limit from various formulations of lattice QCD. Unfortunately, we are not yet in the position to show such a graph. On the contrary, we have even examples where discrepancies seem to be visible when the continuum limit is taken. Let me discuss the situation here at the examples of the nucleon mass and the pseudo scalar decay constant.

3.1 Nucleon mass

For the following discussion, I will use r_0 [33] as a scaling variable. This choice is motivated by the fact that here I am not interested in direct physical values in terms of MeV but only in the scaling behaviour. In addition, determining r_0 is by now a standard and well understood procedure [34] and which is used by many groups. It avoids the difficulty of using the lattice spacing itself which is often determined from different observables in the various collaborations thus leading possibly to large systematic effects.

In the following, an attempt is made to show the continuum limit scaling for the nucleon mass $r_0 M_{\text{nucleon}}$ at fixed pseudo scalar masses $r_0 m_{\text{PS}} = 0.8, 1.0, 1.2$. Let me start with a compilation graph, fig. 6, showing $r_0 M_{\text{nucleon}}$ versus $(r_0 m_{\text{PS}})^2$ as evaluated from a number of collaborations using Wilson, twisted mass, staggered, domain wall and overlap fermions, see the figure caption for corresponding references. The overall impression in this graph is a nice consistency of all the results and a rough scaling behaviour since all results fall into a rather narrow band. Note that in this graph results from $N_f = 2$ and $N_f = 2 + 1$ flavours of quarks are mixed. Of course, it is not too surprising that for the nucleon mass there is no big effect of having a dynamical strange quark.
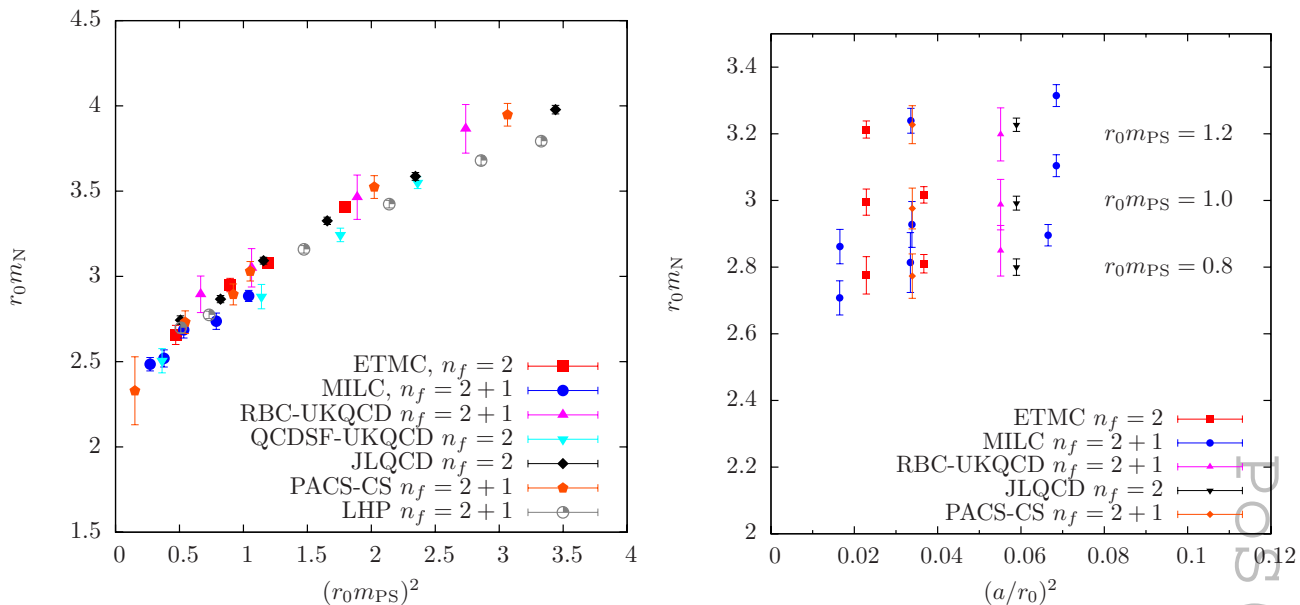
(a) Scatter graph of the nucleon mass as function of the pseudo scalar mass squared using r_0 to set the scale. Data are taken from maximally twisted mass fermions, ref. [6] (ETMC), rooted staggered fermions, ref. [7, 8] (MILC), domain wall fermions, ref. [9] (RBC-UKQCD), non-perturbatively improved Wilson fermions, ref. [12] (QCDSF-UKQCD) and ref. [10] (PACS-CS), overlap fermions, ref. [17, 35] and domain wall fermions on rooted staggered sea quarks, ref. [11] (LHP). A number of values presented in the graph are from private communications.

(b) The nucleon mass as a function of the lattice spacing squared at fixed values of $r_0 m_{PS}$. For explanations what kind of fermions is used, see the left panel of the graph.

**Figure 6:** The scaling behaviour of the nucleon mass.

The scaling behaviour is shown in more detail in fig. 6(b) where the nucleon mass is plotted as a function of $(a/r_0)^2$ for three values of $r_0 m_{PS}$. The data follow basically the expected a^2 behaviour and are consistent with each other.

In summary, for the nucleon sector the scaling properties look promising and with results at more values of the lattice spacing, as will be obtained in the near future, a detailed scaling comparison can be performed.

3.2 The pseudo scalar decay constant

In fig. 7(a) a compilation of various results for $r_0 f_{PS}$ versus $(r_0 m_{PS})^2$ is shown. This graph is very surprising and, at least to me, rather scary. In contrast to the corresponding compilation graph for the nucleon mass in fig. 6, the data for $r_0 f_{PS}$ scatter a lot and do not show a common scaling behaviour.

The cause of the apparent inconsistencies shown in fig. 7(a) is not clear presently. One possible reason could be that for a number of formulations, such as Wilson fermions a renormalization of f_{PS} is required. I therefore show in fig. 7(b) the scaling of $r_0 f_{PS}$ for only those lattice fermion formulations for which an explicit renormalization is not required, i.e. staggered, maximally twisted
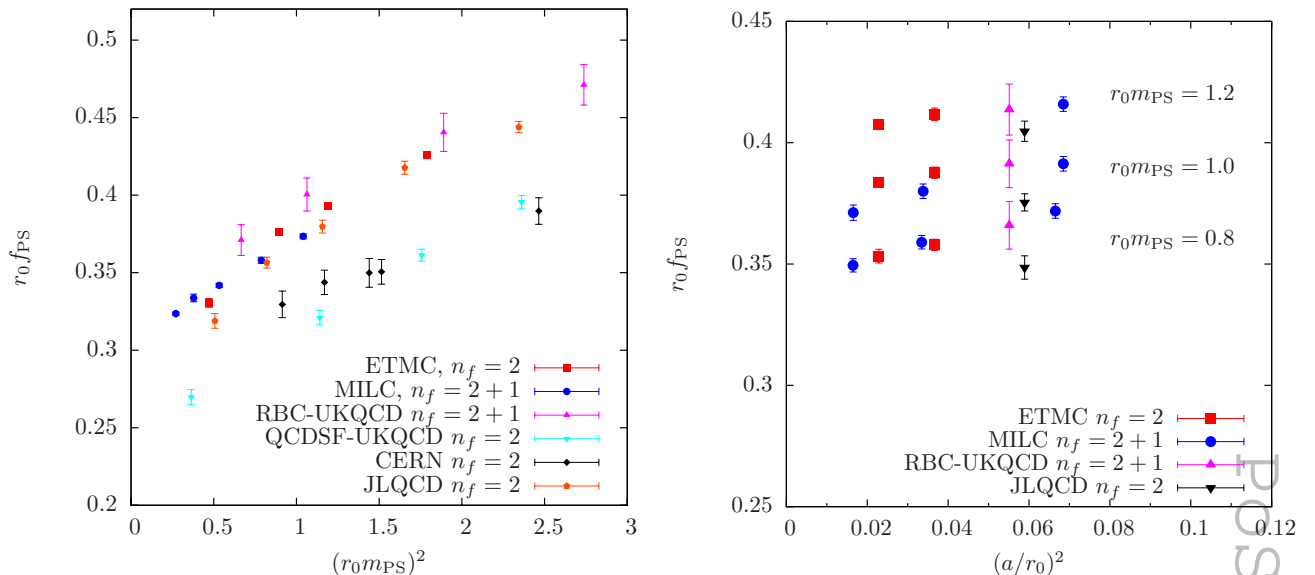
(a) Scatter graph of the pseudo scalar decay constant as function of the pseudo scalar mass squared using r_0 to set the scale. Data are taken from maximally twisted mass fermions, ref. [14, 15] (ETMC), rooted staggered fermions, ref. [36] (MILC), domain wall fermions, ref. [9] (RBC-UKQCD), non-perturbatively improved Wilson fermions, ref. [37] (QCDSF-UKQCD) and ref. [38] (CERN) and overlap fermions [39] (JLQCD). A number of values are taken from private communications of the various collaborations.

(b) The scaling in the lattice spacing of the pseudo scalar decay constant as function of the lattice spacing squared at fixed $r_0 m_{PS}$. Only those formulations of lattice QCD are taken for which no explicit renormalization is necessary.

Figure 7: Lattice spacing scaling of the pseudo scalar decay constant.

mass and overlap fermions. Here the situation looks indeed better and a rough consistency among these results can be seen.

Of course, this does not mean that it is indeed the renormalization of f_{PS} that is behind the very visible differences for f_{PS} from different fermions. This is in particular so, since precise non-perturbative computations of Z_A are available [40]. Other causes could be the values of r_0 used in the comparison and finite size effects can be significant in f_{PS} as is discussed also below, although in the analysis used here the data for f_{PS} were finite size corrected. Another possibility is that the values of the lattice spacing might be still too coarse. Finally, it might be that we see a problem with f_{PS} and seemingly not with m_N because the data for f_{PS} are much more precise and that only such an accuracy can reveal lattice spacing artefacts, i.e. that there might still be large O(a^2) effects.

Which of the above mentioned possibilities will turn out to be the culprit in the end, or whether there is a completely different cause, is not possible to say at the moment. However, I think that the lattice community must investigate this issue in the future. For me, a clarification of the problem with f_{PS} should be high position on the priority list.

4. The actions

In the introductory section I have given two examples of precision *continuum* calculations

coming from lattice QCD simulations, namely the classical benchmark computation of the baryon spectrum and the accurate determination of low energy constants of chiral perturbation theory.

These nice results, however, do not mean that we have lattice QCD fully under control yet. A striking example is the lattice spacing scaling of the pseudo scalar decay constant discussed above. As argued already, a most important point is therefore the verification of universality. The lattice formulations of QCD used today all have their shortcomings each leading to a number of systematic effects and only reaching consistent continuum results from alternative formulations will show that such systematic errors are under control. Let us go shortly through a number of different formulations of lattice fermions and discuss their shortcomings.

4.1 Wilson fermions

Wilson fermions [29] with improvement terms [41] and non-perturbative improvement [42, 43] are used widely in lattice calculations. Their major drawback –besides the demanding computation of the non-perturbative operator improvement– is the explicit breaking of chiral symmetry at non-vanishing values of the lattice spacing. In the past, when using the quenched approximation, one of the consequences was the appearance of unphysical, small eigenvalues of the Wilson-Dirac operator.

With modern simulations of lattice QCD employing the quarks as dynamical degrees of freedom, it turns out, however, that these small eigenmodes do not appear even when much smaller values of the pseudo scalar mass are simulated than it was possible in the quenched approximation. In fact, in ref. [38] a stability criterion has been developed,

$$m_{\rm PS}L \geq \sqrt{3\sqrt{2}aB/Z} \qquad (4.1)$$

providing a bound on the pseudo scalar mass down to which stable simulations can be performed. In eq. (4.1), B is a low energy constant of chiral perturbation theory related to the scalar condensate and Z the quark mass renormalization constant. This bound derives from the observation that there is a spectral gap and from the demand that this gap is, say, three times larger than the width of the corresponding eigenvalue distribution.

In recent years, another feature of Wilson type fermions has been observed. When approaching, for sufficiently large values of the gauge coupling β, the chiral limit at zero quark mass, a rather strong first order phase transition occurs. This phenomenon is a remnant of the continuum first order phase transition when changing the quark mass from positive to negative values.

The lattice distorted first order phase transition has been anticipated already in ref. [44]. First signs of such a phase transition have been seen in refs. [45, 46, 47, 4] and thorough numerical investigations have been performed in refs. [48, 49, 50, 51, 52, 53] in the twisted mass formulation. These numerical findings are in accord with results from chiral perturbation theory, see refs. [44, 54, 55, 56, 57, 58, 59, 60], and a complete picture resulted from these works. As an aside, we also mention that at small values of β an Aoki phase [61] with a spontaneous breaking of parity appears [62, 63].

The strength of the first order phase transition strongly depends on the value of the lattice spacing and of the twisted mass used in the simulation. It is clearly visible at rather coarse lattice spacings and can there even invalidate the stability criterion discussed above. This is demonstrated
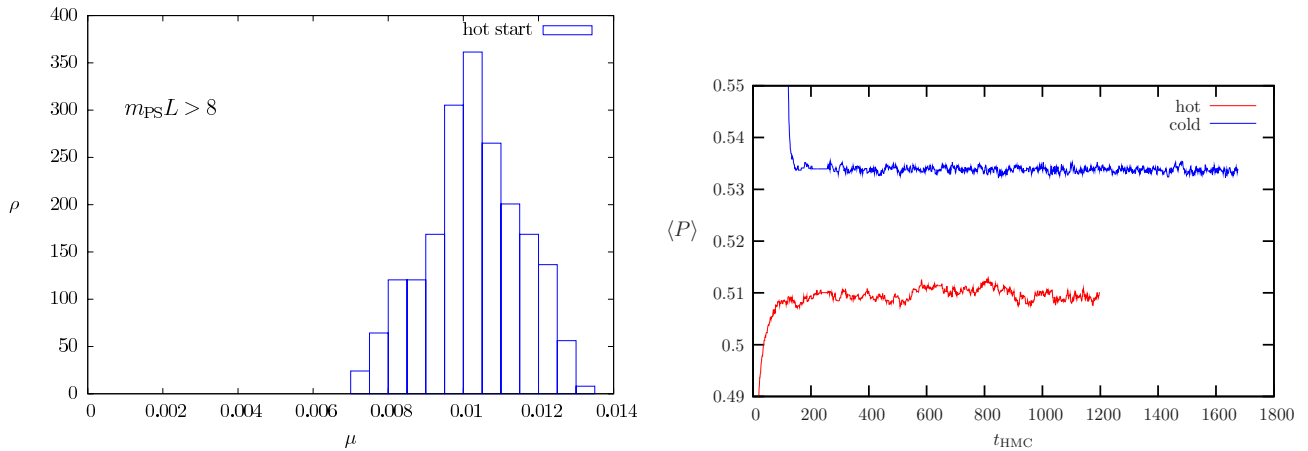
(a) Eigenvalue distribution of the (Hermitean) Wilson-Dirac operator at $\beta = 5.2$ on a 16^4 lattice. The median $\bar{\mu}$ of this distribution is $\bar{\mu} = 0.0103$ while its width σ is $\sigma = 0.0013$ thus obeying the bound given in of eq. (4.1).

(b) The Monte Carlo time history of the plaquette starting from hot and cold configurations. The parameters are the same as those in the left panel. A clear metastable behaviour is observed.

Figure 8: First order phase transition and stability [64].

in fig. 8 [64]. From the width of the eigenvalue distribution shown in fig. 8(a) in the left panel one would conclude that the simulations are stable and safe. However, in the right panel, fig. 8(b), a metastable behaviour of the simulation is observed when starting with hot and cold configurations. Thus, this simulation point, although fulfilling the stability criterion, suffers from metastable behaviour. Let me remark that the value of the lattice spacing used in this investigation has been large, $a > 0.1$fm.

Although with decreasing lattice spacing for fixed twisted mass (zero or non-zero) the effects of the first order phase transition gets weaker and the stability criterion may become more relevant, I still think that it is not sufficient to *only* check the median and the width of the eigenvalue distribution but to also check for the existence of a possible first order phase transition. Checks on both the existence of meta stabilities and the stability criterion from the eigenvalue distribution at the actual simulations points have become routine for a number of collaborations already. As a result of such checks, Wilson fermions are in the fortunate situation that by respecting the bound in eq. (4.1) and avoiding meta stabilities, e.g. by going to sufficiently small lattice spacings, simulations can be expected to be performed and controlled even when applied at pseudo scalar masses as small as 200MeV or even at the physical point.

4.2 Staggered fermions

The staggered fermion community is comprised of mainly the MILC collaboration [65], at least as far as the generation of gauge field configurations is concerned. MILC has by now produced a large and impressive set of configurations with dynamical up and down as well as strange quark degrees of freedom. These configurations are also uploaded to the International Lattice Data Grid (ILDG). (See ref. [66] for a recent overview on ILDG.) MILC has produced these configurations in a project which is ongoing now for many years and has produced configurations at small values of the lattice spacing of $a = 0.06$fm and correspondingly large lattice sizes with $64^3 \cdot 144$ number

of lattice points to obtain a reasonable box size in physical units. There are furthermore plans for future runs with a lattice spacing of $a = 0.045$fm.

Therefore, the question whether this approach to lattice QCD has a conceptual flaw when taking the fourth root is of the greatest importance. The last years have seen many discussions on the issue, see refs. [4, 67, 68, 69, 70] for reviews on the subject. The locality of rooted staggered fermions is addressed in Shamir's work [71, 72]. A controversial and still ongoing debate can be found in refs. [73, 74, 75, 76, 77, 78] and refs. [79, 80, 81, 82, 83, 84, 85]. It is not the aim of this contribution to enter this debate or to even judge between the opponents. However, the picture that emerges –at least to my understanding– can be summarized in two scenarios.

In scenario one, the *practitioner scenario*, we do not insist that we reach the *chiral limit* at zero quark mass for non-zero values of the lattice spacing. Rather, we follow a procedure to stop at some threshold quark mass for a given value of the lattice spacing and then first perform the continuum limit and only afterwards the extrapolation to the physical point. A discussion using staggered chiral perturbation theory to obtain bounds on such threshold quark mass values can be found in refs. [86, 84]. A summary of these results is that for applying *continuum* chiral perturbation theory the taste splitting of staggered fermions has to be much smaller than the lightest pseudo scalar mass. If instead staggered chiral perturbation theory is applied, the taste splitting can be at the order of the lightest pseudo scalar mass, since the taste breaking effects can then be taken into account. For example [87], at a lattice spacing of $a \approx 0.06$fm the lightest pseudo scalar mass simulated is about $m_{PS} = 220$MeV which is three times larger than the observed taste splitting. For $a \approx 0.125$fm the lightest pseudo scalar mass of 250MeV is about the order of the taste splitting and it would thus make not much sense to simulate even smaller masses. More general bounds on the quark mass that follow from the locality considerations of rooted staggered fermions can be found in [72]. A nice discussion of the question of interchanging continuum and chiral limits is given in [88] for the case of the 1-flavour Schwinger model.

In scenario two, the *theorist scenario*, we want to explore the behaviour of staggered fermions with the fourth root trick at or very close to the chiral point. This could reveal some non-perturbative effects of the fourth root trick (e.g. related to the 't Hooft vertex) which could eventually lead to a failure of this approach to lattice QCD. However, when respecting the bounds on the quark mass discussed above, the possible difficulties of rooted staggered fermions in the chiral limit may not affect the results obtained following scenario one. Possible quantities to explore the extreme chiral regime are those related to instanton physics. In my opinion, the exploration of the chiral limit for staggered fermions is of theoretical importance and further scientific discussions, beyond the literature given above, on the topic are certainly welcome. An investigation on this topic can be found in [89].

Another disturbing observation about present staggered fermion simulations is the fact that for the very large lattice simulations an inexact Hybrid Monte Carlo algorithm is used. The inexactness comes from the fact that no accept/reject step is applied at the end of a molecular dynamics trajectory. Although there are some arguments and investigations that this might be a harmless procedure [21], doubts are legitimate and re-introducing the accept/reject step would certainly enlarge the trust in the staggered fermion simulations.

PoS(LATTICE 2008)010

	β	$a\mu_q$	R_O
af_{PS}	3.90	0.004	0.04(06)
	4.05	0.003	$-0.03(06)$
am_V	3.90	0.004	0.02(07)
	4.05	0.003	$-0.10(11)$
af_V	3.90	0.004	$-0.07(18)$
	4.05	0.003	$-0.31(29)$
am_Δ	3.90	0.004	0.022(29)
	4.05	0.003	$-0.004(45)$

Table 1: Examples of relative differences between charged and neutral operator expectation values, $R_O = (O^\pm - O^0)/O^\pm$, measuring the isospin breaking effects in twisted mass lattice QCD.

4.3 Twisted mass fermions

Twisted mass fermions at maximal twist [30, 90] have by now proved to be a practical and successful tool for performing lattice QCD simulations, see e.g. refs. [14, 91, 92, 93, 6, 94, 95] and contributions to this conference [96, 97, 98, 99, 16, 100]. The expected $O(a)$-improvement [30] has been demonstrated for many observables by now in the quenched approximation [101, 102, 103, 104] as well as employing dynamical quarks [14, 15, 105, 93]. In particular, it was shown that stable simulations down to pseudo scalar masses of about $m_{PS} \approx 260$MeV are possible.

Twisted mass fermions share with standard Wilson fermion the drawback of breaking chiral symmetry at any non-zero lattice spacing. An additional major drawback of twisted mass fermions is the explicit violation of isospin symmetry at non-zero values of the lattice spacing. From the simulations by the European twisted mass collaboration (ETMC) there are two basic observations concerning this lattice artefact. The first is that the isospin breaking, although consistent with the expected $O(a^2)$ scaling, is large when the mass difference of the charged and the neutral pseudo scalar mass is considered as can be seen in fig. 9(a). Note that for the computation of the neutral pseudo scalar mass disconnected diagrams need to be taken into account. In contrast, the scaling behaviour of the charged pseudo scalar mass is very flat showing almost no lattice artefacts as demonstrated in fig. 9(b). Thus, the large lattice artefact seen in fig. 9(a) must be due to the neutral pseudo scalar mass alone.

A second observation is that other quantities seem not to be affected by the isospin violation, as can be seen from table 1. There the relative difference of charged and neutral quantities, $R_O = (O^\pm - O^0)/O^\pm$ turns out to be compatible with zero, at least within the errors.

The two observations described above find an interpretation in terms of the Symanzik effective theory analysis [106]. In particular, there it can be shown that the charged pseudo scalar mass receives only $O(a^2 m_\pi^2, a^4)$ corrections while the neutral pseudo scalar mass has corrections at $O(a^2)$. This explains the scaling behaviour of the masses shown in fig. 9. The results listed in table 1 must then correspondingly be interpreted that in these quantities the neutral pseudo scalar mass (or related quantities) do not play a dominant role.

14
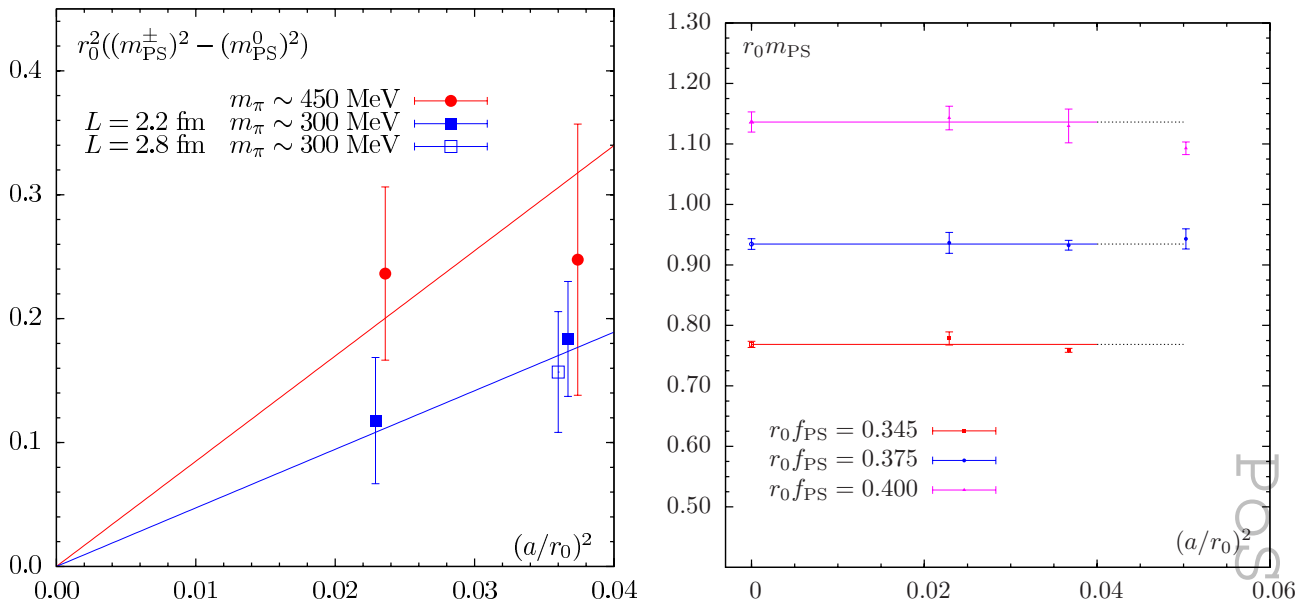
(a) The difference of the charged and neutral pseudo scalar mass as a function of a^2 in the twisted mass formulation of lattice QCD at different values of the charged pseudo scalar mass. A large $O(a^2)$ lattice artefact is observed.

(b) The scaling behaviour of the charged pseudo scalar mass at fixed values of the pseudo scalar decay constant. The scaling behaviour is basically flat in a^2 demonstrating that the cutoff effect in the left panel originates solely from the neutral pseudo scalar mass.

Figure 9: Isospin violations for twisted mass fermions at the example of the charged and neutral pseudo scalar masses.

Whether the Symanzik type analysis provides the correct interpretation of the numerically obtained results or whether other interpretations are possible and, maybe, more applicable is presently being investigated by ETMC. In any case, there exists no general argument, whether or not large isospin breaking effects can appear in certain quantities. Although there exist indications that large isospin breaking effects may only appear in certain observables (like the neutral pion mass), this issue must be studied carefully on a case by case basis by any group employing twisted mass fermions.

4.4 Smearing

Many simulations use nowadays some method of smearing of the links [107, 108, 109] that enter the lattice-Dirac operator. This procedure has the advantage to smooth out the configurations seen by the lattice Dirac operator. As a consequence, the condition number can be reduced and also the gauge field fluctuations are suppressed leading to possibly faster and more stable simulations compared to the case when no smearing is employed. In addition, also the effects of the first order phase transition mentioned above seem to be diminished [110].

An open question is of course, to what extent smearing should be used. Performing only moderate smearing as done in e.g. refs. [111, 112] will presumably not affect the simulations much. However, already one level of stout smearing [107] leads in perturbation theory [113] to values for the renormalization constants and improvement coefficients that are close to their tree-

level values when smearing is employed [111, 114]. This holds at least for certain values of the smearing parameter $\rho \approx 0.1$.

When many levels of smearing are performed as used in ref. [115], there is the danger that uncontrolled systematic effects emerge as the Dirac operator may become quite non-local. In the simulation, which revealed the baryon spectrum shown in fig. 2, 6-levels of stout smearing had been used [13]. Many concerns about a possible alteration of the short distance behaviour of physical quantities have been put forward by this rather high level of smearing and a suspicion that the action is too non-local has been raised. The BMW collaboration themself has performed a locality test following the principle idea of ref. [116]. Note that a locality test of the Dirac-operator itself will not reveal any non-local effects since it anyway acts on nearest neighbours only.

Therefore, the quantity investigated has been the response of the Dirac operator $D(x,y)$ with respect to a gauge link variation $\|\partial D(x,y)/\partial U_\mu(x+z)\|$ as a function of the distance z/a. With a smearing parameter ρ chosen to be well below one, it can be expected that smearing effects decay like ρ^n and hence the effects of smearing vanish rapidly for increasing distances. However, it is important to realize that there is a high degree of degeneracy of lattice points at large distances which become relevant through the smearing procedure. In addition, in most quantities the behaviour of the inverse fermion matrix (propagator) matters, not of the fermion matrix itself. This might strongly increase the effect of a high level smearing. Thus it is unclear what the net effect of smearing will be.

The outcome of the locality test by the BMW collaboration is shown in fig. 10(a). For this test three different values of the lattice spacing were used as indicated in the graph. The data demonstrates that there is an exponentially fast decay of the norm of the variation of the lattice Dirac operator with respect to the gauge field $U_\mu(x+z)$ as a function of z/a. Thus, an action with 6-levels of stout smearing still shows an exponential localization. In this respect, it is similar to the locality properties of overlap fermions. Therefore, although a strict transfer matrix is missing when high-levels of smearing are performed, the action can be considered as being local in the field theoretical sense. It might still be that certain short distance quantities, such as the scalar condensate, renormalization factors or the Coulomb part of the static potential are affected by smearing. But, so far there is no convincing evidence for such a distortion. The positive –and, maybe, rather surprising– outcome of the locality investigation of the BMW collaboration suggests that it would be very worthwhile to investigate high-level stout smearing further on and test or rule out possible conceptual shortcomings.

4.5 Fermions with exact/approximate lattice chiral symmetry

Domain wall fermions

Domain wall fermions [117, 118] are *only* chiral invariant in the limit of an *infinite* extra dimension. They are theoretically on the same footing (see ref. [119] and references therein) as overlap fermions [120, 32, 121]. It is important to realize that truncating the number of slices in the extra dimension is equivalent to reduce, e.g., the degree of the polynomial when constructing the overlap operator. In both ways chirally improved actions are obtained. However, chiral symmetry will be broken explicitly, the effects of which ought to be studied. For domain wall fermions such
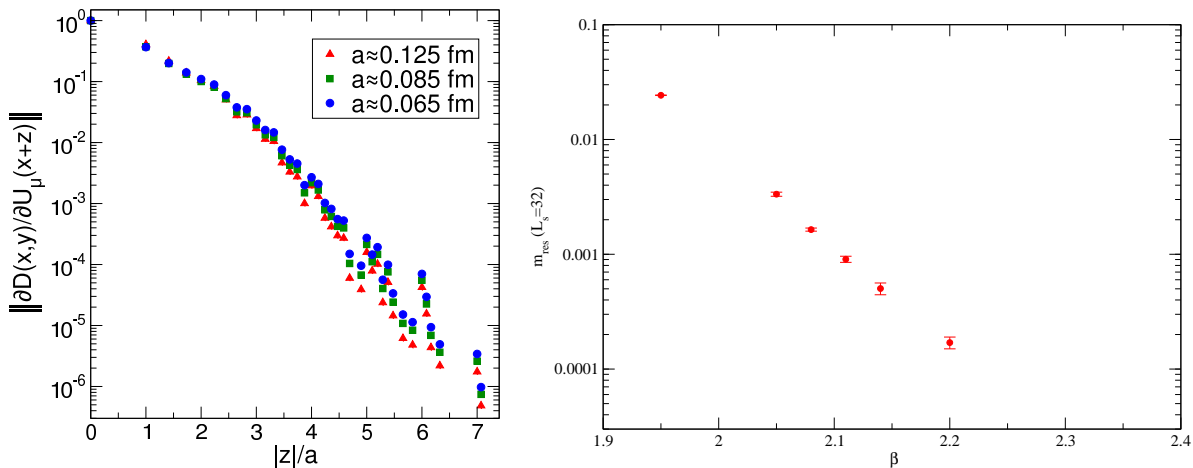
(a) The response of the Wilson Dirac operator on a variation of a gauge field at a distance z/a. The graph illustrates that locality is realized with an exponentially fast decrease of the norm of $\|\partial D(x,y)/\partial U_\mu(x+z)\|$.

(b) The residual mass m_{res} at fixed value of the extra dimension, $L_s = 32$, as a function of the gauge coupling β. Note the logarithmic scale indicating the exponentially fast vanishing of m_{res}.

Figure 10: Effects of smearing on the locality (left panel). The behaviour of the residual mass as function of β (right panel).

investigations have been performed by the RBC-UKQCD collaborations in refs. [122, 123, 9]. The outcome of these investigations is that chirality breaking effects can essentially be quantified by the size of the residual quark mass in relation to the quark mass values employed in the simulations. When comparing the residual mass m_{res} with the sea and valence quark masses in recent domain wall simulations, at a coarse value of the lattice spacing, m_{res} is dangerously close to the sea quark mass and even bigger than the valence quark mass. However, for smaller lattice spacing the situation improves considerably. It is worth to stress that domain wall fermion simulations are not too much more expensive than Wilson-type fermion simulations as illustrated in fig. 4(a). In addition, algorithmic tricks such as inexact deflation or multigrid ideas can also be applied for domain wall fermions thus leading to possibly large improvement factors.

One interesting observation from recent domain wall simulations is the behaviour of the residual mass as a function of the lattice spacing. As fig. 10(b) shows, for a fixed value of the number of slices in the extra dimension L_s the residual mass vanishes exponentially fast with decreasing lattice spacing. Since the residual mass is proportional to the eigenvalue density at zero eigenvalues, this means that at some value of β the topological charge will not change anymore. A corresponding observation has been made by groups using the overlap operator [124]. These findings are a consequence of the fact that at small enough values of the lattice spacing, the plaquette bound for the existence of a spectral gap of the Wilson-Dirac operator of ref. [116] is satisfied leading to a spectral gap of the corresponding kernel Dirac operator and therefore no topology change can occur. This can lead to a severe conceptual problem for overlap or domain wall fermion simulations. The spectral gap itself on the other hand is a consequence of the negative bare quark mass employed in the kernel operator. For standard Wilson-type fermions, the bare quark mass is on the other hand positive and hence the above arguments do not apply. Of course, this does not exclude that also

standard Wilson-type fermions can run into problems with topology changes at large values of β.

Overlap fermions

The statement that the cost for overlap or domain wall fermions with *exact* lattice chiral symmetry is at least one order of magnitude larger than for Wilson or staggered fermions, is, unfortunately still true today (see e.g. ref. [125]) although many developments and improvements have already been taken place. The reasons are the nested iterations in inverting the operator and the difficulty to tunnel between different topological charge sectors.

Nevertheless, simulations on small lattices are performed nowadays and some first results are emerging [126, 127, 128, 129, 130]. However, it seems to me that chiral invariant simulations in lattice QCD are still a subject for the future[1].

Fixed topology simulations

As a solution to the topology tunneling problem of overlap simulations, the usage of topology fixing actions has been put forward since these actions avoid by construction the problem with topology changes. Earlier attempts to use a modified gauge action to fix topology did not lead to satisfactory results since it was not possible to fix topology completely when values of the lattice spacings, say, $a \approx 0.1$fm were aimed at [135, 136].

As an alternative approach, the usage of a determinant ratio,

$$R = \det \left[D_W^2(-m_0) \right] / \det \left[D_W^2(-m_0) + \mu^2 \right] \tag{4.2}$$

has been proposed in ref. [137]. This constitutes another local modification of the gauge action since the masses used in eq. (4.2) are taken to be large. In particular, the bare quark mass of the Wilson Dirac operator D_W is taken to be negative which suppresses the occurrence of small eigenvalues, forbidding therefore topology changes. A number of overlap fermion simulations employing the determinant ratio of eq. (4.2) have already been performed [138, 139, 140, 35]. An account of present simulations employing the determinant ratio is given in ref. [124].

In this still rather new approach to lattice QCD a number of issues have to be clarified such as a test of the topological finite size effects [141, 142], the ergodicity of the simulations and possibly long auto correlations. Nevertheless, I find this a very interesting way of obtaining the continuum limit: in the continuum, the total topological charge will average out to zero, while local topological charges will, of course, still appear. Thus, it is a valid and intriguing approach to fix topology to zero from the very beginning and see how the system behaves towards the continuum limit. From my point of view, this offers a nice alternative for QCD simulations.

4.6 Other approaches

There are more alternatives of lattice QCD formulations, such as FLIC fermions [143], chirally

---

[1]Note, however, that in chiral invariant Higgs-Yukawa like models which employ the overlap operator [131, 132, 133, 134] lattices with size $32^3 \cdot 64$ are used already.

improved fermions [144], perfect action fermions [145] and Hyp-link smearing techniques [112]. Simulations with these kind of fermions have not yet reached as ambitious parameter values as many of the large collaborations employ and which use the fermion formulations discussed above.

4.7 Summary of action discussion

There are a number of interesting fermion actions on the market. Each of them has certain shortcomings the most important of which are:

O(a)-*improved Wilson fermions*: breaking of chiral symmetry, non-perturbative operator improvement;

rooted staggered fermions: taste breaking, non-local lattice action;

twisted mass fermions: breaking of chiral symmetry, isospin breaking;

overlap fermion: expense of simulation;

domain wall fermions: expense of simulation and breaking of chirality;

smearing: effects of high levels of smearing;

fixed topology: topological finite size effects.

It seems that there is no ideal action which is obvious to select. Therefore, just to re-iterate, a universality test showing which of these actions lead to consistent continuum limit values is a necessity.

5. Chiral perturbation theory

The fact that nowadays pseudo scalar masses below 300MeV can be reached, offers the possibility to confront the numerically obtained data with the corresponding expressions from chiral perturbation theory. It is important to realize that the values for the low energy constants obtained from fits to chiral perturbation theory can be used in return for many phenomenological applications by inserting them into the relevant formulae of chiral perturbation theory. Thus a reliable and precise calculation of the low energy constants is a most valuable outcome of lattice simulations. In consequence, studying the mass dependence of many physical quantities in lattice QCD is important and, of course, actively pursued.

When discussing chiral perturbation theory in the context of lattice simulations one has to specify the setup in which the discussion is taking place. There are essentially three cases, (i) SU(2) chiral perturbation theory applicable to $N_f = 2$ mass degenerate quarks, (ii) the corresponding SU(3) case and (iii) the case where we have light, mass-degenerate up and down quarks and a strange quark at its physical value.

5.1 SU(2) chiral perturbation theory

The classical quantities to confront with chiral perturbation theory are the pseudo scalar mass and the pseudo scalar decay constant which can be determined very precisely from lattice QCD simulations. When a range of quark masses is considered that corresponds to an interval of pseudo scalar masses of $250 \lesssim m_{PS} \lesssim 450$MeV then it seems that the 1-loop chiral perturbation theory formula (see refs. [146, 147] for the adequate fitting formulae) is applicable as seen in the examples shown in fig. 3(a) (from ETMC) and fig. 3(b) (from the JLQCD collaboration). In fact, the data are described by the 1-loop expression so well that there is no room for any sensitivity for the

2-loop corrections. Fig. 3(b) also demonstrates that going beyond pseudo scalar masses of, say, 450MeV the chiral fits become problematic since fits using alternative expansion parameters lead to significant differences.

A conclusion that for SU(2) chiral perturbation theory the 1-loop formula for the above given mass range is satisfactory is, however, possibly pre-mature. Examples are the vector and the charged radii of the pseudo scalar particle as computed by JLQCD [148] and ETMC [149]. Here, a 1-loop chiral perturbation theory formula cannot describe the data appropriately and a NNLO correction has to be taken into account. This holds true, even if the same range of pseudo scalar masses is used for which the quark mass dependence of f_{PS} and m_{PS} are described perfectly by NLO chiral perturbation theory.

It is an open question, as to whether the failure to describe the pion radii by the 1-loop expression of chiral perturbation is due to the fact that even for $250 \lesssim m_{PS} \lesssim 450$MeV the 2-loop correction is necessary or, whether the zero quark mass asymptotics of different observables is qualitatively different. To answer this question, presumably many quantities have to be fitted simultaneously such that the 2-loop low energy constants can be reliably determined. Having the LECs in our hand, it will then become possible to quantify the 2-loop corrections for given values of the pseudo scalar mass.
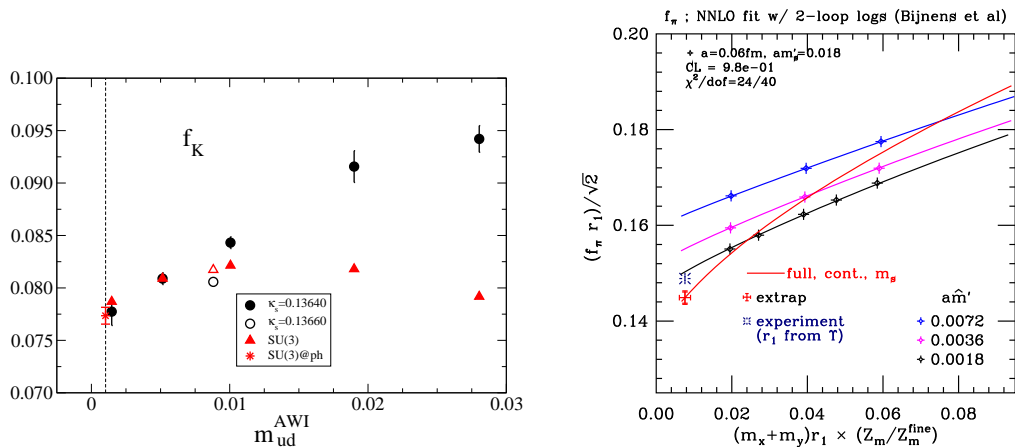
5.2 SU(3) chiral perturbation theory

Up to my knowledge there has been so far no attempt to perform dedicated simulations with $N_f = 3$ mass degenerate quarks to compare with chiral perturbation theory [150, 151]. In my opinion such simulations would, however, be important for two reasons. The first is obviously that we want to compare the low energy constants from a SU(3) chiral perturbation theory fit to the corresponding case of SU(2). The second is that for the non-perturbative renormalization of $N_f = 2 + 1$ lattice QCD simulations preferably a massless renormalization scheme should be used which requires simulations at a number of quark masses employing $N_f = 3$ mass degenerate flavours and then to perform an extrapolation to the chiral point. Such simulations would automatically generate the set of data to confront to SU(3) chiral perturbation theory and are planned by e.g. by the MILC collaboration [152].

5.3 $N_f = 2 + 1$

In most simulations we have the situation that 2 mass degenerate up and down quarks and a strange quark close to its physical value are employed. The simulations are then performed by varying the light quark masses while keeping the strange quark mass roughly constant in physical units.

Attempts to describe then the mass dependence of the pseudo scalar decay constant up to the Kaon scale by SU(3) chiral perturbation theory [153] are not successful. In fig. 11(a) we give an example from the PACS-CS collaboration [10, 154, 155] which shows the comparison of the Kaon decay constant f_K to NLO chiral perturbation theory. Clearly, there is a large discrepancy between the measured values from the lattice simulations and chiral perturbation theory. The description of the numerical data breaks down rather early in the quark mass and any attempt to extend the formulae up to the strange quark mass fails. Such a behaviour is also observed by other collaborations:

(a) Applying NLO SU(3) chiral perturbation theory to the Kaon decay constant f_K (from the PACS-CS collaboration). A clear discrepancy between the numerical data and chiral perturbation theory predictions can be observed.

(b) Application of continuum NNLO chiral perturbation theory to staggered fermion simulations at a value of the lattice spacing of $a \approx 0.06$fm.

Figure 11: Chiral perturbation theory for $N_f = 2 + 1$.

the RBC-UKQCD collaboration [9, 156] uses an effective Kaon chiral perturbation theory to fix the problem; in the case of staggered fermions, the lattice artefact corrections are taken into account [157] which enlarges, however, the set of parameters to be fitted substantially. But still, a NLO formula from chiral perturbation theory does not seem to be sufficient to describe the numerical data up to the Kaon scale. It is therefore tried to use [158] *continuum* NNLO chiral perturbation theory for the smallest value of the lattice spacing of $a = 0.06$fm for staggered fermion simulations. This is shown in fig. 11(b). Since further simulations at an even smaller value of the lattice spacing are planned (or even already ongoing) this offers a nice way to reduce the number of free parameters and test the applicability of chiral perturbation theory in the continuum.

To summarize, for $N_f = 2$ mass degenerate flavours of quarks chiral perturbation theory seems to work very well, although it is not clear whether the NLO formula is applicable for all quantities. The situation when adding the strange quark mass is problematic and a simple application of chiral perturbation theory does not work. Here, some input and interaction with experts from chiral perturbation theory is highly welcome.

6. Some additional issues

6.1 Mixed actions

In order to compute physical observables, often a mixed action approach is used. Here, the kind of lattice fermions used for generating the configurations, the *sea quarks*, is different from the kind of lattice fermions used to compute the propagators, *the valence quarks*. Such a procedure is particularly useful, if we think of computationally very expensive fermions such as overlap or domain wall fermions and if 'wrong chirality' mixings in the twisted mass regularization are to be tackled [159]. In order to relate valence and sea quarks, an appropriate matching condition ought

21

to be applied. To this end, typically the bare parameters of the valence quark action is tuned in such a way that the pseudo scalar mass of sea and valence quarks match. Keeping such a matching condition towards the continuum limit will then give a unitary theory in the continuum limit, at least if the lattice sea and valence quark actions were unitary by themselves.

Although such a mixed action approach is therefore conceptually sound, it is not studied in great detail yet. In particular, for any non-zero value of the lattice spacing very special lattice artefacts can appear. For example, the scalar correlator can become negative and the lattice spacing corrections towards the continuum limit can get additional contributions from the fact that the sea and the valence quark masses are different [160, 161, 162, 163, 164, 165, 166].

To illustrate that care has to be taken in this mixed action approach I give two examples. The first is a calculation of overlap valence quarks on a maximally twisted mass sea [167] at a value of the lattice spacing of about $a \approx 0.09$fm. While matching the pseudo scalar mass, the values of the pseudo scalar decay constants show a remarkable discrepancy at the matching point, $af_{PS}^{tm} = 0.0646(4)$ while $af_{PS}^{overlap} = 0.077(4)$. Another example is a domain wall valence computation on a rooted staggered sea [11] at a value of the lattice spacing of about $a \approx 0.124$fm. Again matching the pseudo scalar mass, a significant difference in the nucleon mass is found: $aM_{nucleon}^{staggered} = 0.723(6)$ while $aM_{nucleon}^{domainwall} = 0.696(7)$. Since in the continuum limit the values of physical observables have to agree, these two examples hint at rather large lattice artefacts appearing in a mixed action setup. Thus, a careful check of lattice artefacts will be very useful and is almost mandatory. Note, however, that for closely related actions such as Osterwalder-Seiler quarks [168] on a twisted mass sea [169] or unrooted staggered valence on rooted staggered sea fermions, physical observables seem to match better.

Fortunately, the lattice spacing effects in a number of mixed action formulations have been analyzed in lattice chiral perturbation theory [160, 161, 162, 164, 170, 171, 172]. These formulae can and have been used to describe the numerical data.

6.2 Non-perturbative renormalization

Doubtlessly, non-perturbative renormalization is a necessity in lattice QCD simulations. This can be illustrated with the example of the strange quark mass, which obtains a value of $m_{strange}^{perturbative} = 72 \pm 2 \pm 9$MeV while $m_{strange}^{nonperturbative} = 105 \pm 3 \pm 9$MeV [91]. Note that the values of the perturbative renormalized strange quark mass taken here from ETMC is fully consistent with the corresponding PACS-CS result [10]. A similar picture emerges for the light quark masses.

In order to obtain the non-perturbatively evaluated renormalization constants in a *mass independent* renormalization scheme, either the RI-MOM [173] or the Schrödinger functional (SF) scheme [174, 175] can be used. In the former case, an extrapolation to the chiral limit has to be performed, while in the second case the theory can be simulated directly at or close to zero quark masses.

For the case of $N_f = 2$ mass degenerate quarks such procedures have been already successfully applied, see [176]. For the case of $N_f = 2 + 1$, there is the additional complication that the strange quark mass is kept close to its physical value. Therefore, in order to obtain a massless renormalization scheme, additional runs with $N_f = 3$ mass degenerate quarks would have to be performed in principle. Such simulations are not available yet but e.g. MILC is planning such runs [152].
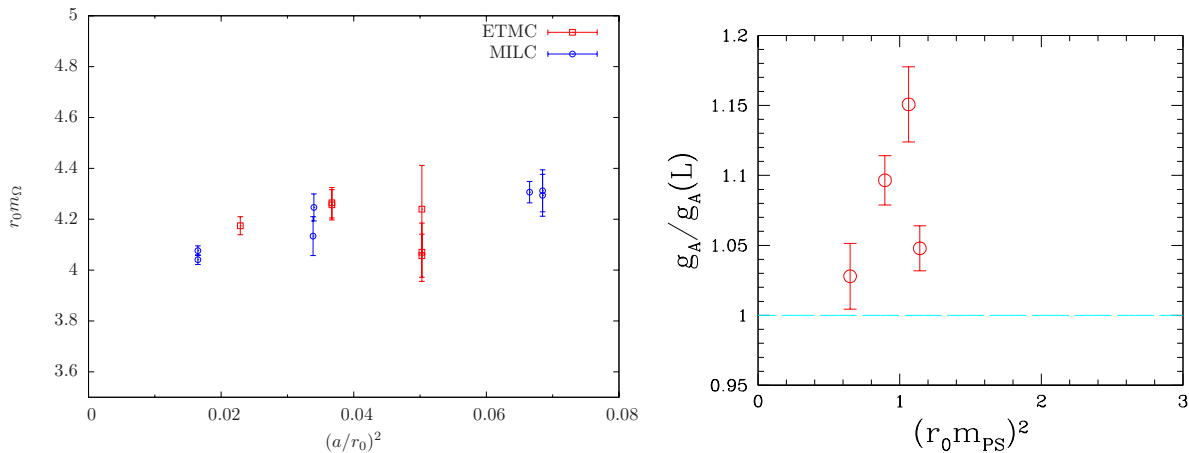
(a) Omega mass at fixed value $r_0 m_{PS}$ as a function of a^2. Data are from MILC (having a dynamical strange) and ETMC (with only up and down sea quarks).

(b) Finite size effects for g_A as determined by the QCDSF collaboration. The ratio of the infinite volume value g_A and its finite volume analogue $g_A(L)$ can reveal large finite size effects at the 15%-20% level.

Figure 12: Omega mass and finite size effects of g_A.

As mentioned above such simulations have the additional advantage that SU(3) chiral perturbation theory can be checked and eventually the SU(3) low energy constants be extracted.

For the time being, collaborations such as RBC-UKQCD try to estimate the systematic effects coming from a fixed and rather large strange quark mass and add this as a systematic error in the renormalization constants [9]. However, this needs an explicit check. Also, first investigations with the SF scheme and $N_f = 3$ flavours of quarks are under way [177]. For theoretical discussion of SF boundary conditions at this conference see [178, 97].

6.3 Effects of strange quark

Often a question is asked whether the results from $N_f = 2$ flavours of quarks are reliable since the strange quark is neglected and taken only as a valence quark in the calculation of various observables.

In order to see any effects of a dynamical strange quark, a most sensitive quantity should be the Ω baryon which consists of three strange quarks and has no strong decay. In fig. 12(a) results from computations of MILC [8] (which has a dynamical strange quark) and ETMC [179] (which uses only up and down quarks in the sea) for the Ω baryon are compared at various values of the lattice spacing keeping $r_0 m_{PS}$ fixed. Within the error bars, no evidence of an effect of the strange quark mass is seen. To reveal such an effect, presumably the error bars would have to shrink substantially. Up to my knowledge, also in other quantities no evidence (with possibly the exception of f_{D_s}) of the relevance of a dynamical strange quark has been observed so far and it will be interesting to see in the future whether and when such effects show up.

6.4 Finite size effects

Simple mesonic quantities such as m_{PS} and f_{PS} are computed so precisely in present day numerical simulations that effects of a finite volume are clearly visible and become a dominant

systematic error. However, it seems that the analysis performed in ref. [147] provides an adequate description of the finite size effects for m_{PS} and f_{PS} as confirmed by many groups. In particular, if values of $m_{PS}L \gtrsim 3.5$ are used, while keeping L itself large enough to avoid squeezing effects of the wave function [180, 181], the finite size effects are at the percent level and can be fully controlled by applying the formulae of ref. [147].

However, the nice results for these basic mesonic quantities cannot be taken over automatically to other quantities. As demonstrated in fig. 12(b) by the example of g_A (discussed by the QCDSF collaboration [182]), other quantities may have finite volume effects that can reach 15%-20%. Similar finite volume effects were observed for the ratio g_A/g_V by the RBC-UKQCD collaboration. Thus, finite volume effects need to be carefully investigated on a case by case study.

6.5 Topology

The question of topology on the lattice is one of the most interesting and difficult one to address. However, in the last years, we have seen much progress in this direction [183, 184, 185, 186, 187]. As only one example I show in fig. 13(a) the mass dependence of the topological susceptibility towards the chiral limit as obtained by the RBC-UKQCD collaboration. The point I want to make here is that the topological susceptibility shows the right behaviour towards the chiral limit in that it vanishes as we approach massless quarks. This behaviour is also seen from other formulations, see the references given above.

As a second example for a quantity which is directly related to topology, I show in fig. 13(b) the η_2 mass from $N_f = 2$ simulations. The η_2 mass is the analogue of the η' mass for $N_f = 2+1$. Using the much improved algorithms for the simulations, advances of computing disconnected diagrams as well as new methods, it is possible to reach small values of the pseudo scalar mass and small errors for this difficult to compute quantity. The graph, compiled by ETMC, ref. [94], reveals a basically flat behaviour of the η_2 mass as a function of the pseudo scalar mass and confirms that at the physical point a value of the η_2 mass of $M_{\eta_2} \approx 865$MeV can be extracted thus showing a large contribution to the mass by topological effects. Note that with $N_f = 1$ dynamical quarks [188] the corresponding η' (η_1) mass comes out to be 330(20) MeV, in agreement with the Witten-Veneziano formula.

6.6 Getting social

As a last section in this discussion of a number of selected topics concerning lattice QCD simulations, I would like to address the communication within our lattice community. Although a strong competition between various "dynasties" of international collaborations is very welcome, there are, in my opinion, some easy to realize ways to homogenize our efforts and give therefore a more coherent picture to the outside world.

ILDG: It would be very good if all collaborations were willing to upload their configurations to the ILDG. Although there an initial threshold effort, afterwards using ILDG tools become routine and a number of collaborations employ the ILDG tools successfully and efficiently already in their daily work. The usage of the ILDG format for the configurations allows for an easy exchange of configurations that can provide valuable cross checks among different collaborations. See refs. [189, 190, 191, 66] for overviews of ILDG activities.
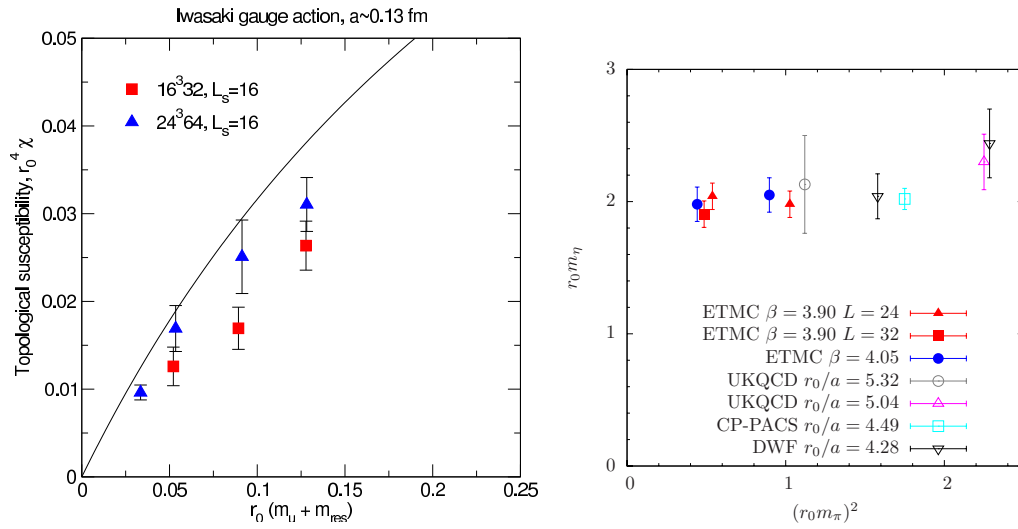
(a) Topological susceptibility from the RBC-UKQCD collaboration in the approach to the chiral limit. In particular, the data on the larger lattice indicate that the topological susceptibility will vanish when massless quarks are reached.

(b) The η_2 mass (the analogue of the η' mass for two flavours of quarks) as a function of the pseudo scalar mass. The flatness in the mass dependence allows an estimate at the physical point of $\eta_2 \approx 865$ MeV.

Figure 13: The topological susceptibility and the η_2 mass.

Codes: The algorithms used for present days simulations have become rather complicated and it is no longer true that it takes a few days to write a Hybrid Monte Carlo code that includes state of the art improvements from scratch. In such a situation, it would be very good if such complicated codes could be made available to the lattice community, preferably as an open source platform such that useful additions can be implemented. Examples of published codes are [192, 193, 194]. Other collaborations are encouraged to follow up on these examples.

Details: As discussed at length in the preceding sections, the results from lattice simulations suffer from a number of systematic effects that have to be controlled as well as possible. In order to be able to judge whether this has been achieved in the work of a particular collaboration, it would therefore be necessary to know about the details of the simulation, the analysis and the estimates of the systematic effects. Therefore, I would like to encourage all the collaborations to not only publish high gloss papers with final results, but also technical papers with all technical details of their work. This will allow everybody to judge and cross-check the results, but may also teach us about the techniques and whether they are of interest for other collaborations. In addition, it would be very useful to publish tables of raw data. Another aspect is to perform blind analyses in order to avoid possible human interfaced biases.

7. Conclusions

The main message of this proceeding is the very substantial progress lattice field theory has achieved in the last years. Due to algorithmic breakthroughs, (see fig. 4), as the major factor in combination with a significant increase of super computer power and conceptual developments, several international collaborations are nowadays performing simulations that were unthinkable

even a few years ago. In particular, in lattice QCD we are now reaching lattice spacing values of $a \approx 0.05$fm, pseudo scalar masses of about 250MeV and below and box sizes with linear extent of $L \approx 3$fm. Using O(a) improved lattice actions allows eventually for controlled continuum, chiral and infinite volume extrapolations. Fig. 1 summarizes the values of the lattice spacing and pseudo scalar masses that are covered in typical simulations presently.

Examples of physical results that are available already now and which are computed as continuum quantities with systematic errors taken into account are the baryon spectrum as represented in fig. 2 and the precise determinations of several low energy constants, see fig. 3. Many more physical results are to be expected in the near future since much of the raw data of lattice QCD, the dynamically generated gauge field configurations, exist already or will be generated soon. They are partly stored on the International Data Grid where they are often freely available.

Despite this undeniable progress, caveats remain. The actions employed for the dynamical simulations lead to systematic errors that need to be controlled such as explicit breaking of chiral symmetry, isospin and taste breaking, high-level of smearing and non-locality. In addition, the various actions show different kind of lattice artefacts. Therefore, a check is needed that different lattice fermion formulations lead to the same continuum limit values and a test of this universality is, in my opinion, one of the most urgent demands in lattice QCD. This problem is highly nontrivial as fig. 7(a) demonstrates: here a compilation of many available lattice results for the pseudo scalar decay constant reveals a warning: no common scaling is observed when different lattice fermions are considered. This is in contrast to the nucleon mass of fig. 6(a) where a good overall lattice spacing scaling can be observed.

There are also a number of open questions that remain to be clarified: how to use chiral perturbation theory when a dynamical strange is fixed at its physical value? Related to this is the question of how best to extrapolate e.g. baryons and other quantities to the physical point. How about the non-perturbative renormalization in the case of $N_f = 2 + 1$ flavours? Can we control the finite volume effects for quantities different from simple mesonic observables? Should we include the charm as a dynamical degree of freedom and what will be the lattice artefacts? How to best treat unstable particles in lattice QCD? These are some of the challenges that the lattice QCD community has to address and solve.

Although there are for sure still a number of obstacles to overcome, lattice QCD simulations have finally become realistic. The physics coming out of such simulations have therefore to be discussed prudently. And, just to finish, it is maybe indeed the time now to make a serious effort towards a lattice particle data booklet.

Acknowledgments

References

[1] K. G. Wilson, Nucl. Phys. Proc. Suppl. **17**, 82 (1990).

[2] R. Tripiccione, Nucl. Phys. Proc. Suppl. **17**, 137 (1990).

[3] C. Bernard *et al.*, Nucl. Phys. Proc. Suppl. **106**, 199 (2002).

[4] K. Jansen, Nucl. Phys. Proc. Suppl. **129**, 3 (2004), [hep-lat/0311039].

[5] PACS-CS Collaboration, these proceedings (2008).

[6] European Twisted Mass, C. Alexandrou *et al.*, Phys. Rev. **D78**, 014509 (2008), [0803.3190].

[7] C. Aubin *et al.*, Phys. Rev. **D70**, 094505 (2004), [hep-lat/0402030].

[8] MILC, C. Bernard *et al.*, PoS **LAT2007**, 137 (2007), [0711.0021].

[9] C. Allton *et al.*, 0804.0473.

[10] PACS-CS, S. Aoki *et al.*, 0807.1661.

[11] A. Walker-Loud *et al.*, 0806.4549.

[12] QCDSF, M. Gockeler *et al.*, PoS **LAT2007**, 129 (2007), [0712.0010].

[13] BMW Collaboration, C. Hoelbling and S. Krieg, these proceedings (2008).

[14] ETM, P. Boucaud *et al.*, Phys. Lett. **B650**, 304 (2007), [hep-lat/0701012].

[15] European Twisted Mass, C. Urbach, PoS **LAT2007**, 022 (2007), [0710.1517].

[16] P. Dimopoulos *et al.*, 0810.2873.

[17] J. Noaki *et al.*, 0810.1360.

[18] C. Urbach, K. Jansen, A. Shindler and U. Wenger, Comput. Phys. Commun. **174**, 87 (2006), [hep-lat/0506011].

[19] M. Luscher, Comput. Phys. Commun. **165**, 199 (2005), [hep-lat/0409106].

[20] L. Del Debbio, L. Giusti, M. Luscher, R. Petronzio and N. Tantalo, JHEP **02**, 056 (2007), [hep-lat/0610059].

[21] D. Toussaint, private communication.

[22] M. A. Clark and A. D. Kennedy, Phys. Rev. **D75**, 011502 (2007), [hep-lat/0610047].

[23] B. Orth, T. Lippert and K. Schilling, Phys. Rev. **D72**, 014503 (2005), [hep-lat/0503016].

[24] N. Christ, C. Jung and E. Scholz, private communication.

[25] M. Luscher, JHEP **12**, 011 (2007), [0710.5417].

[26] RBC and UKQCD, N. Christ and C. Jung, PoS **LAT2007**, 028 (2007).

[27] K. Ishikawa, these proceedings (2008).

[28] N. Christian, K. Jansen, K. Nagai and B. Pollakowski, Nucl. Phys. **B739**, 60 (2006), [hep-lat/0510047].

[29] K. G. Wilson, Phys. Rev. **D10**, 2445 (1974).

[30] R. Frezzotti and G. C. Rossi, JHEP **08**, 007 (2004), [hep-lat/0306014].

[31] W. Bietenholz and U. J. Wiese, Nucl. Phys. **B464**, 319 (1996), [hep-lat/9510026].

[32] H. Neuberger, Phys. Lett. **B417**, 141 (1998), [hep-lat/9707022].

[33] R. Sommer, Nucl. Phys. **B411**, 839 (1994), [hep-lat/9310022].

[34] S. Necco and R. Sommer, Nucl. Phys. **B622**, 328 (2002), [hep-lat/0108008].

[35] H. Ohki *et al.*, 0806.4744.

[36] C. Bernard *et al.*, PoS **LAT2007**, 090 (2007), [0710.1118].

[37] M. Gockeler *et al.*, PoS **LAT2006**, 160 (2006), [hep-lat/0610071].

[38] L. Del Debbio, L. Giusti, M. Luscher, R. Petronzio and N. Tantalo, JHEP **02**, 082 (2007), [hep-lat/0701009].

[39] JLQCD, J. Noaki *et al.*, PoS **LAT2007**, 126 (2007), [0710.0929].

[40] M. Della Morte, R. Sommer and S. Takeda, 0807.1120.

[41] B. Sheikholeslami and R. Wohlert, Nucl. Phys. **B259**, 572 (1985).

[42] ALPHA, K. Jansen and R. Sommer, Nucl. Phys. **B530**, 185 (1998), [hep-lat/9803017].

[43] CP-PACS, S. Aoki *et al.*, Phys. Rev. **D73**, 034501 (2006), [hep-lat/0508031].

[44] S. R. Sharpe and J. Singleton, R., Phys. Rev. **D58**, 074501 (1998), [hep-lat/9804028].

[45] T. Blum *et al.*, Phys. Rev. **D50**, 3377 (1994), [hep-lat/9404006].

[46] JLQCD, S. Aoki *et al.*, Nucl. Phys. Proc. Suppl. **106**, 263 (2002), [hep-lat/0110088].

[47] JLQCD, S. Aoki *et al.*, hep-lat/0409016.

[48] F. Farchioni *et al.*, Eur. Phys. J. **C39**, 421 (2005), [hep-lat/0406039].

[49] F. Farchioni *et al.*, Nucl. Phys. Proc. Suppl. **140**, 240 (2005), [hep-lat/0409098].

[50] F. Farchioni *et al.*, Eur. Phys. J. **C42**, 73 (2005), [hep-lat/0410031].

[51] F. Farchioni *et al.*, PoS **LAT2005**, 072 (2006), [hep-lat/0509131].

[52] F. Farchioni *et al.*, Eur. Phys. J. **C47**, 453 (2006), [hep-lat/0512017].

[53] F. Farchioni *et al.*, Phys. Lett. **B624**, 324 (2005), [hep-lat/0506025].

[54] S. R. Sharpe and J. M. S. Wu, Phys. Rev. **D71**, 074501 (2005), [hep-lat/0411021].

[55] S. Aoki and O. Bär, Phys. Rev. **D70**, 116011 (2004), [hep-lat/0409006].

[56] S. R. Sharpe and J. M. S. Wu, Phys. Rev. **D70**, 094029 (2004), [hep-lat/0407025].

[57] G. Munster and C. Schmidt, Europhys. Lett. **66**, 652 (2004), [hep-lat/0311032].

[58] G. Münster, JHEP **09**, 035 (2004), [hep-lat/0407006].

[59] G. Münster, C. Schmidt and E. E. Scholz, Nucl. Phys. Proc. Suppl. **140**, 320 (2005), [hep-lat/0409066].

[60] L. Scorzato, Eur. Phys. J. **C37**, 445 (2004), [hep-lat/0407023].

[61] S. Aoki, Phys. Lett. **B190**, 140 (1987).

[62] A. Sternbeck, E.-M. Ilgenfritz, W. Kerler, M. Müller-Preußker and H. Stüben, Nucl. Phys. Proc. Suppl. **129**, 898 (2004), [hep-lat/0309059].

[63] E.-M. Ilgenfritz, W. Kerler, M. Müller-Preußker, A. Sternbeck and H. Stüben, Phys. Rev. **D69**, 074511 (2004), [hep-lat/0309057].

[64] K. Jansen and C. Urbach, unpublished (2008).

[65] *MILC home page*, http://www.physics.indiana.edu/ sg/milc.html.

[66] T. Yoshie, these proceedings (2008).

[67] D. H. Adams, Nucl. Phys. Proc. Suppl. **140**, 148 (2005), [hep-lat/0409013].

[68] S. Durr, PoS **LAT2005**, 021 (2006), [hep-lat/0509026].

[69] S. R. Sharpe, PoS **LAT2006**, 022 (2006), [hep-lat/0610094].

[70] A. S. Kronfeld, PoS **LAT2007**, 016 (2007), [0711.0699].

[71] Y. Shamir, Phys. Rev. **D71**, 034509 (2005), [hep-lat/0412014].

[72] Y. Shamir, Phys. Rev. **D75**, 054503 (2007), [hep-lat/0607007].

[73] M. Creutz, PoS **LAT2006**, 208 (2006), [hep-lat/0608020].

[74] M. Creutz, Phys. Lett. **B649**, 241 (2007), [0704.2016].

[75] M. Creutz, PoS **LAT2007**, 007 (2007), [0708.1295].

[76] M. Creutz, Annals Phys. **323**, 2349 (2008), [0711.2640].

[77] M. Creutz, 0804.4307.

[78] M. Creutz, Phys. Rev. **D78**, 078501 (2008), [0805.1350].

[79] M. Golterman, Y. Shamir and B. Svetitsky, Phys. Rev. **D74**, 071501 (2006), [hep-lat/0602026].

[80] C. Bernard, M. Golterman, Y. Shamir and S. R. Sharpe, Phys. Lett. **B649**, 235 (2007), [hep-lat/0603027].

[81] C. Bernard, M. Golterman and Y. Shamir, Phys. Rev. **D73**, 114511 (2006), [hep-lat/0604017].

[82] C. Bernard, M. Golterman and Y. Shamir, PoS **LAT2006**, 205 (2006), [hep-lat/0610003].

[83] C. Bernard, M. Golterman, Y. Shamir and S. R. Sharpe, Phys. Rev. **D77**, 114504 (2008), [0711.0696].

[84] C. Bernard, M. Golterman and Y. Shamir, Phys. Rev. **D77**, 074505 (2008), [0712.2560].

[85] C. Bernard, M. Golterman, Y. Shamir and S. R. Sharpe, 0808.2056.

[86] C. Bernard, Phys. Rev. **D73**, 114503 (2006), [hep-lat/0603011].

[87] C. Bernard and M. Golterman, private communication.

[88] S. Durr and C. Hoelbling, Phys. Rev. **D71**, 054501 (2005), [hep-lat/0411022].

[89] D. H. Adams, Phys. Rev. **D77**, 105024 (2008), [0802.3029].

[90] R. Frezzotti and G. C. Rossi, JHEP **10**, 070 (2004), [hep-lat/0407002].

[91] European Twisted Mass, B. Blossier *et al.*, JHEP **04**, 020 (2008), [0709.4574].

[92] K. Cichy, J. Gonzalez Lopez, K. Jansen, A. Kujawa and A. Shindler, Nucl. Phys. **B800**, 94 (2008), [0802.3637].

[93] ETM, P. Boucaud *et al.*, 0803.0224.

[94] ETM, K. Jansen, C. Michael and C. Urbach, 0804.3871.

[95] A. Shindler, Phys. Rept. **461**, 37 (2008), [0707.4093].

[96] ETM, K. Jansen, C. Michael, A. Shindler and M. Wagner, 0808.2121.

[97] J. G. Lopez, K. Jansen and A. Shindler, (2008), [0810.0620].

[98] K. Jansen, A. Nube and A. Shindler, 0810.0300.

[99] ETM, P. Dimopoulos, C. McNeile, C. Michael, S. Simula and C. Urbach, 0810.1220.

[100] R. Baron *et al.*, PoS **LATTICE2008**, 094 (2008), [0810.3807].

[101] K. Jansen, A. Shindler, C. Urbach and I. Wetzorke, Phys. Lett. **B586**, 432 (2004), [hep-lat/0312013].

[102] K. Jansen, M. Papinutto, A. Shindler, C. Urbach and I. Wetzorke, Phys. Lett. **B619**, 184 (2005), [hep-lat/0503031].

[103] K. Jansen, M. Papinutto, A. Shindler, C. Urbach and I. Wetzorke, JHEP **09**, 071 (2005), [hep-lat/0507010].

[104] A. M. Abdel-Rehim, R. Lewis and R. M. Woloshyn, Phys. Rev. **D71**, 094505 (2005), [hep-lat/0503007].

[105] ETM, P. Dimopoulos, R. Frezzotti, G. Herdoiza, C. Urbach and U. Wenger, PoS **LAT2007**, 102 (2007), [0710.2498].

[106] R. Frezzotti and G. Rossi, PoS **LAT2007**, 277 (2007), [0710.2492].

[107] C. Morningstar and M. J. Peardon, Phys. Rev. **D69**, 054501 (2004), [hep-lat/0311018].

[108] S. Durr, 0709.4110.

[109] A. Hasenfratz, R. Hoffmann and S. Schaefer, JHEP **05**, 029 (2007), [hep-lat/0702028].

[110] K. Jansen *et al.*, PoS **LAT2007**, 036 (2007), [0709.4434].

[111] R. Horsley, H. Perlt, P. E. L. Rakow, G. Schierholz and A. Schiller, 0807.0345.

[112] S. Schaefer, A. Hasenfratz and R. Hoffmann, PoS **LAT2007**, 132 (2007), [0709.4130].

[113] S. Capitani, S. Durr and C. Hoelbling, JHEP **11**, 028 (2006), [hep-lat/0607006].

[114] R. Horsley, P. E. L. Rakow, H. Perlt, G. Schierholz and A. Schiller, 0809.4769.

[115] S. Durr *et al.*, 0802.2706.

[116] P. Hernandez, K. Jansen and M. Lüscher, Nucl. Phys. **B552**, 363 (1999), [hep-lat/9808010].

[117] D. B. Kaplan, Phys. Lett. **B288**, 342 (1992), [hep-lat/9206013].

[118] V. Furman and Y. Shamir, Nucl. Phys. **B439**, 54 (1995), [hep-lat/9405004].

[119] Y. Kikukawa, Prepared for 30th International Conference on High-Energy Physics (ICHEP 2000), Osaka, Japan, 27 Jul - 2 Aug 2000.

[120] P. H. Ginsparg and K. G. Wilson, Phys. Rev. **D25**, 2649 (1982).

[121] H. Neuberger, Phys. Lett. **B427**, 353 (1998), [hep-lat/9801031].

[122] RBC and UKQCD, C. Allton *et al.*, Phys. Rev. **D76**, 014504 (2007), [hep-lat/0701013].

[123] RBC, D. J. Antonio *et al.*, Phys. Rev. **D77**, 014509 (2008), [0705.2340].

[124] JLQCD Collaboration, S. Hashimoto, these proceedings (2008).

[125] S. Schaefer, PoS **LAT2006**, 020 (2006), [hep-lat/0609063].

[126] T. DeGrand, Z. Liu and S. Schaefer, Phys. Rev. **D74**, 094504 (2006), [hep-lat/0608019].

[127] T. DeGrand and S. Schaefer, Phys. Rev. **D76**, 094509 (2007), [0708.1731].

[128] N. Cundy, these proceedings (2008).

[129] N. Cundy, S. Krieg, T. Lippert and A. Schafer, PoS **LAT2007**, 030 (2007), [0710.1785].

[130] N. Cundy, S. Krieg, T. Lippert and A. Schafer, 0803.0294.

[131] P. Gerhold and K. Jansen, PoS **LAT2007**, 075 (2007), [0710.1106].

[132] Z. Fodor, K. Holland, J. Kuti, D. Nogradi and C. Schroeder, PoS **LAT2007**, 056 (2007), [0710.3151].

[133] P. Gerhold and K. Jansen, JHEP **10**, 001 (2007), [0707.3849].

[134] P. Gerhold, these proceedings (2008).

[135] H. Fukaya, S. Hashimoto, T. Hirohashi, K. Ogawa and T. Onogi, Phys. Rev. **D73**, 014503 (2006), [hep-lat/0510116].

[136] W. Bietenholz *et al.*, JHEP **03**, 017 (2006), [hep-lat/0511016].

[137] JLQCD, H. Fukaya *et al.*, Phys. Rev. **D74**, 094505 (2006), [hep-lat/0607020].

[138] JLQCD and TWQCD, S. Aoki *et al.*, Phys. Lett. **B665**, 294 (2008), [0710.1130].

[139] JLQCD, S. Aoki *et al.*, Phys. Rev. **D77**, 094503 (2008), [0801.4186].

[140] JLQCD, S. Aoki *et al.*, 0803.3197.

[141] R. Brower, S. Chandrasekharan, J. W. Negele and U. J. Wiese, Phys. Lett. **B560**, 64 (2003), [hep-lat/0302005].

[142] S. Aoki, H. Fukaya, S. Hashimoto and T. Onogi, Phys. Rev. **D76**, 054508 (2007), [0707.0396].

[143] S. Boinpolli *et al.*, Int. J. Mod. Phys. **A22**, 5053 (2007).

[144] C. Gattringer *et al.*, 0809.4514.

[145] A. Hasenfratz, P. Hasenfratz, F. Niedermayer, D. Hierl and A. Schafer, PoS **LAT2006**, 178 (2006), [hep-lat/0610096].

[146] J. Gasser and H. Leutwyler, Phys. Lett. **B184**, 83 (1987).

[147] G. Colangelo, S. Dürr and C. Haefeli, Nucl. Phys. **B721**, 136 (2005), [hep-lat/0503014].

[148] JLQCD, T. Kaneko *et al.*, PoS **LAT2007**, 148 (2007), [0710.2390].

[149] ETMC, S. Simula, PoS **LAT2007**, 371 (2007), [0710.0097].

[150] J. Gasser and H. Leutwyler, Phys. Rept. **87**, 77 (1982).

[151] J. Gasser and H. Leutwyler, Ann. Phys. **158**, 142 (1984).

[152] MILC, U. Heller, (2008), private communication.

[153] J. Gasser and H. Leutwyler, Nucl. Phys. **B250**, 465 (1985).

[154] PACS-CS, N. Ukita *et al.*, 0810.0563.

[155] PACS-CS, D. Kadoh *et al.*, 0810.0351.

[156] RBC and UKQCD, E. E. Scholz, 0809.3251.

[157] C. Aubin and C. Bernard, Phys. Rev. **D73**, 014515 (2006), [hep-lat/0510088].

[158] C. Bernard, private communication.

[159] R. Frezzotti and G. C. Rossi, Nucl. Phys. Proc. Suppl. **128**, 193 (2004), [hep-lat/0311008].

[160] O. Bar, G. Rupak and N. Shoresh, Phys. Rev. **D67**, 114505 (2003), [hep-lat/0210050].

[161] O. Bar, C. Bernard, G. Rupak and N. Shoresh, Phys. Rev. **D72**, 054502 (2005), [hep-lat/0503009].

[162] O. Bar, G. Rupak and N. Shoresh, Phys. Rev. **D70**, 034508 (2004), [hep-lat/0306021].

[163] S. Prelovsek, C. Dawson, T. Izubuchi, K. Orginos and A. Soni, Phys. Rev. **D70**, 094503 (2004), [hep-lat/0407037].

[164] M. Golterman, T. Izubuchi and Y. Shamir, Phys. Rev. **D71**, 114508 (2005), [hep-lat/0504013].

[165] O. Bar, K. Jansen, S. Schaefer, L. Scorzato and A. Shindler, PoS **LAT2006**, 199 (2006), [hep-lat/0609039].

[166] C. Aubin, J. Laiho and R. S. Van de Water, Phys. Rev. **D77**, 114501 (2008), [0803.0129].

[167] N. Garron and L. Scorzato, PoS **LAT2007**, 083 (2007), [0710.1582].

[168] K. Osterwalder and E. Seiler, Ann. Phys. **110**, 440 (1978).

[169] A. Vladikas, these proceedings (2008).

[170] J.-W. Chen, D. O'Connell, R. S. Van de Water and A. Walker-Loud, Phys. Rev. **D73**, 074510 (2006), [hep-lat/0510024].

[171] J.-W. Chen, D. O'Connell and A. Walker-Loud, Phys. Rev. **D75**, 054501 (2007), [hep-lat/0611003].

[172] J.-W. Chen, D. O'Connell and A. Walker-Loud, 0706.0035.

[173] G. Martinelli, C. Pittori, C. T. Sachrajda, M. Testa and A. Vladikas, Nucl. Phys. **B445**, 81 (1995), [hep-lat/9411010].

[174] M. Luscher, R. Narayanan, P. Weisz and U. Wolff, Nucl. Phys. **B384**, 168 (1992), [hep-lat/9207009].

[175] K. Jansen *et al.*, Phys. Lett. **B372**, 275 (1996), [hep-lat/9512009].

[176] R. Sommer, hep-lat/0611020.

[177] Y. Taniguchi, these proceedings (2008).

[178] B. Lederer and S. Sint, these proceedings (2008).

[179] V. Drach, these proceedings (2008).

[180] M. Fukugita, H. Mino, M. Okawa and A. Ukawa, Phys. Rev. Lett. **68**, 761 (1992).

[181] M. Fukugita, H. Mino, M. Okawa, G. Parisi and A. Ukawa, Phys. Lett. **B294**, 380 (1992).

[182] A. A. Khan *et al.*, Phys. Rev. **D74**, 094508 (2006), [hep-lat/0603028].

[183] JLQCD and TWQCD, T. W. Chiu *et al.*, 0810.0085.

[184] T. DeGrand and S. Schaefer, 0712.2914.

[185] U. Wenger, these proceedings (2008).

[186] C. Bernard *et al.*, PoS **LAT2007**, 310 (2007), [0710.3124].

[187] S. Durr, Z. Fodor, C. Hoelbling and T. Kurth, JHEP **04**, 055 (2007), [hep-lat/0612021].

[188] F. Farchioni *et al.*, 0810.0161.

[189] A. Ukawa, Nucl. Phys. Proc. Suppl. **140**, 207 (2005), [hep-lat/0409084].

[190] K. Jansen, PoS **LAT2006**, 013 (2006), [hep-lat/0609012].

[191] C. E. Detar, PoS **LAT2007**, 009 (2007), [0710.1660].

[192] *M. Lüscher home page*, http://luscher.web.cern.ch/luscher/.

[193] USQCD, B. Joo, J. Phys. Conf. Ser. **125**, 012066 (2008), [0806.2312].

[194] A. Borici, hep-lat/0610054.